PHR1 and PHL1 mediate rapid high-light responses and acclimation to high photosynthetic activity

Lukas Ackermann[1], Agnes Fekete[2], Laura Schröder[3], Thomas Nägele[3], Alina J. Hieber[1], Monika Müller[1], Martin J. Mueller[2], Maria Klecker[1*]

[1] Plant Physiology, University of Bayreuth, 95447 Bayreuth, Germany

[2]Julius-von-Sachs-Institute of Biosciences, Biocenter, Pharmaceutical Biology, University of Würzburg, 97082 Würzburg, Germany

[3]Faculty of Biology, Plant Evolutionary Cell Biology, LMU München, 82152 Planegg, Germany

[*]Address correspondence to: Maria Klecker, Department of Plant Physiology, University of Bayreuth, Universitätsstrasse 30, D-95447 Bayreuth, Germany. e-mail: maria.klecker@uni-bayreuth.de

ORCID IDs

Maria Klecker	0000-0001-5508-2363
Lukas Ackermann	0009-0009-8604-6029
Agnes Fekete	0000-0003-3058-7570
Martin J. Mueller	0000-0001-8122-5460
Thomas Nägele	0000-0002-5896-238X
Alina J. Hieber	0009-0009-0407-8968

ABSTRACT

- Rapid acclimation towards high light is vital for the prevention of phototoxic stress to plant tissues. Photosynthesis transiently consumes inorganic phosphate (P_i). We therefore asked whether changes in intracellular P_i pools can act as a signal for reprogramming gene expression upon increased light intensity.

- The function of triose phosphate utilization for intracellular P_i homeostasis was deciphered by investigation of mutants defective in both photoassimilate partitioning and low-P_i signaling. Next, we determined subcellular P_i levels and transcript accumulation upon short-term high light. Physiological consequences were examined by analyses of ATP, carbohydrates, and an untargeted lipid profiling approach.

- The capacity for triose phosphate utilization clearly affected systemic P_i signaling. High-light treatment caused a rapid depletion specifically of chloroplast P_i levels paralleled by induction of transcripts dependent on PHOSPHATE STARVATION RESPONSE 1 (PHR1) and PHR1-LIKE 1. Among the high-light induced targets of PHR1, *SRG3/GDPD1* is involved in phospholipid catabolism. Lipid profiling revealed differences between WT and *srg3* mutant plants upon high light, including changes in linolenic acid and photoprotective zeaxanthin.

- We conclude that photosynthetic activity regulates the low-P_i response machinery in the nucleus to implement high-light acclimation. This facilitates the liberation of cellular P as well as the maintenance of membrane lipid integrity.

Key words

PHR1, phosphate starvation, light acclimation, photosynthesis, glycerophosphodiester phosphodiesterase, membrane remodeling, non-photochemical quenching (NPQ)

Introduction

Light energy is provided to photoautotrophic organisms at variable intensities that can fall below or exceed the requirements of the photosynthetic machinery at unpredictable times during the day period. This necessitates an enzymatic machinery capable of coping with rapid changes in metabolic flux, as well as the containment of overexcitation-induced hazards, such as lipid peroxidation (Havaux & Niyogi, 1999). Both challenges are met not only by post-

55 transcriptional regulation of enzyme activity (reviewed in König et al. (2012), Matiolli et al.
56 (2022)), but also by pronounced changes in mRNA abundance that occur within 30 minutes
57 upon an increase in irradiance (Vogel *et al.*, 2014; Suzuki *et al.*, 2015; Huang *et al.*, 2019). The
58 latter mechanism depends on fast signal transmission between the chloroplast and the nuclear
59 transcription machinery. Such communication is mediated by 'primary' retrograde signals
60 (Dietz, 2015), including redox cues and reactive oxygen species which are produced during
61 photosynthetic reactions (Bechtold *et al.*, 2008; Dietz *et al.*, 2016). Additionally, increased
62 electron transport activity and light-induced Calvin-Benson cycle activation promote the
63 accumulation of primary products of carbon fixation (Dietz & Heber, 1984, 1986; Borghi *et al.*,
64 2019) which may themselves act as signaling molecules (Häusler *et al.*, 2014; Moore *et al.*,
65 2014). Hence, induction of high-light specific gene expression partially depends on the triose
66 phosphate/phosphate translocator (TPT) that mediates the exchange of triose phosphates and 3-
67 phosphoglycerate (3-PGA) with inorganic phosphate (P_i) at the chloroplast envelope (Schneider
68 *et al.*, 2002; Vogel *et al.*, 2014; Weise *et al.*, 2019). A central function of the TPT in light
69 acclimation and retrograde signaling was corroborated by the severe high-light dependent
70 phenotypes of double mutants defective in *TPT* and *ADG1* (for *ADP GLUCOSE*
71 *PYROPHOSPHORYLASE 1*), encoding a small subunit of the ADP-glucose pyrophosphorylase
72 complex (AGPase) which is required for the biosynthesis of transitory starch (Schmitz *et al.*,
73 2012). Phenotypes of *adg1-1 tpt* double mutants include growth retardation, low diurnal
74 changes in carbohydrate levels, and high chlorophyll fluorescence. These observations point
75 towards an important role of photosynthate partitioning for retrograde signaling, however the
76 identity of the primary sensors as well as signal transduction mechanisms are still unclear.

77 Phosphorus makes up about 2-30 permille of the plant dry mass (Kumar *et al.*, 2019),
78 as it is incorporated into a large subset of biomolecules. Systemic signaling of P_i availability
79 and P_i distribution within the plant body mainly depend on a conserved gene family encoding
80 PHOSPHATE STARVATION RESPONSE 1 (PHR1) and at least 14 PHR1 LIKE (PHL)
81 transcription factors of the GARP coiled-coiled type (Rubio *et al.*, 2001; Zhou *et al.*, 2008;
82 Bustos *et al.*, 2010; Thibaud *et al.*, 2010; Sun *et al.*, 2016; Safi *et al.*, 2017). Simultaneous loss
83 of *PHR1* and *PHL1* function affects the expression of roughly 70 % of the P_i starvation
84 responsive genes in the shoots of Arabidopsis (*Arabidopsis thaliana)* (Bustos *et al.*, 2010). A
85 decrease in cellular P_i concentration impairs production of the inositol pyrophosphate species
86 InsP8 in the cytosol, relieving PHR1/PHLs of suppression by SPX (for SYG1/Pho81/XPR1)
87 domain-containing proteins, thus linking transcription factor activity to P_i availability (Puga *et*
88 *al.*, 2014; Dong *et al.*, 2019; Zhu *et al.*, 2019; Ried *et al.*, 2021). The transcriptional response

89 to P_i scarcity leads to scavenging of external and internal P_i sources through phosphatase
90 induction (Morcuende *et al.*, 2007) and altered lipid metabolism (Misson *et al.*, 2005; Pant *et*
91 *al.*, 2015; Yang *et al.*, 2025), anthocyanin biosynthesis (Nilsson *et al.*, 2012; Liu *et al.*, 2022;
92 Li *et al.*, 2023), and protection from photodamage (Nilsson *et al.*, 2012), to name a selection.
93 The largest pool of cellular P reserves resides in the vacuole, and it has been shown in rice
94 (*Oryza sativa*), that vacuolar P_i efflux into the cytosol is mediated by two proteins of the
95 glycerol 3-phosphate transporter family which are transcriptionally induced by PHR proteins
96 (Xu *et al.*, 2019). Three homologs have been identified in Arabidopsis and are termed VPE1-3
97 (Ramaiah *et al.*, 2011; Xu *et al.*, 2019), but their contribution to P_i homeostasis has not been
98 addressed so far in dicotyledonous plants. PHR1/PHLs are characterized as transcriptional
99 activators (Nilsson *et al.*, 2007; Bustos *et al.*, 2010). Accordingly, direct targets of PHR1
100 (Bustos *et al.*, 2010; Castrillo *et al.*, 2017) are strongly upregulated upon P_i starvation and
101 include genes such as *PHOSPHATE STARVATION-INDUCED GENE 2* (*PS2*; AT1G73010)
102 (Hanchi *et al.*, 2018), *MONOGALACTOSYLDIACYLGLYCEROL SYNTHASE 3* (*MGD3*;
103 AT2G11810) (Kobayashi *et al.*, 2004), and *GLYCEROPHOSPHODIESTER*
104 *PHOSPHODIESTERASE 1/SENESCENCE-RELATED GENE 3* (*GDPD1/SRG3*; AT3G02040)
105 (Cheng *et al.*, 2011). The latter encodes a plastid-localized enzyme with broad-spectrum
106 glycerophosphodiester phosphodiesterase activity releasing primary alcohols and glycerol
107 3-phosphate from deacylated phospholipids (Cheng *et al.*, 2011). SRG3 is supposed to mainly
108 act in the catalysis of phosphatidylcholine to provide glycerol-3-phosphate for DGDG
109 biogenesis, for glycolytic utilization, or liberation of P_i by subsequent acid phosphatase activity
110 (Cheng *et al.*, 2011). A function in phospholipid homeostasis was recently corroborated by
111 Wojciechowska et al. (2024) who proposed that the transcriptional repressor PROTODERMAL
112 FACTOR2 directly links phospholipid availability to the repression of both *SRG3* and *SPX1*.
113 The *SRG3* gene was shown to be important for seedling fitness and maintenance of cellular P_i
114 levels under P_i starvation conditions (Cheng *et al.*, 2011), but how exactly SRG3 contributes to
115 nutrient homeostasis is not understood.

116 P_i is unique among the macronutrients in that it is the only root-supplied element which
117 is directly required for photosynthesis (Heldt & Rapley, 1970; Dietz & Heber, 1984). It has
118 been shown experimentally that under high-CO_2 and high-light conditions, photosynthesis can
119 indeed become limited by P_i supply to the chloroplast, both under P_i depleted and nutrient-rich
120 conditions (Walker & Osmond, 1986; Dietz & Foyer, 1986; Sivak & Walker, 1986). However,
121 whether rapid increase in photosynthetic activity directly affects P_i homeostasis of the cell, is
122 still unclear. In this study, we show that increments in light intensity rapidly deplete chloroplast

123 P_i reserves *in planta*. Strikingly, although other cellular P_i pools are not affected by short-term
124 high light, this is accompanied by a nuclear transcriptional response characteristic of P_i
125 depletion which depends on *PHR1* and *PHL1*. Transcript analysis of the *adg1 tpt-2* mutant links
126 PHR(-like) activation to triose phosphate allocation. Processes regulated by PHR1/PHL1 upon
127 high light contribute to photosynthetic acclimation since *phr1 phl1* mutants are sensitive to
128 high-light growth conditions, and showed altered carbohydrate and anthocyanin accumulation
129 compared to the wildtype (WT) when the light intensity was increased. Moreover, analyses of
130 the starch biosynthesis-deficient *adg1 phr1 phl1* triple mutant revealed an important function
131 of P_i signaling when triose phosphate utilization is constrained. Induction of genes involved in
132 lipid metabolism such as *SRG3* by PHR1/PHL1 furthermore contributes to fatty acid
133 homeostasis and membrane photoprotection, as revealed by lipid profiling of the *srg3* mutant
134 upon high light. Together, we propose that PHR1/PHL1 mediate cellular P_i release and rapid
135 photosynthetic acclimation upon increases in light intensity, probably activated by direct
136 sensing of chloroplast P_i levels upon triose phosphate overproduction.

137 # Results

138 **Triose phosphate utilization affects P_i signaling**

139 Photoassimilate allocation and utilization in the chloroplast and cytosol are supposed to
140 limit the rate of P_i recycling from photosynthetic products (McClain & Sharkey, 2019). In line
141 with this assumption, P_i deprivation has been shown to stimulate starch accumulation in a
142 *PHR1*-dependent manner, which involves AGPase activity (Nilsson *et al.*, 2007). To address
143 whether partitioning of phosphorylated assimilates contributes to P_i homeostasis of the cell, we
144 examined the phenotypes of mutants defective in starch biosynthesis (*adg1-1*) and chloroplastic
145 triose phosphate export (*tpt-2*) during P_i starvation in the presence of 14.61 mM (0.5 %) sucrose.
146 Starch accumulation in response to P_i depletion was abolished in both the *phr1-3 phl1* double
147 mutant and the *adg1-1* mutant (Figure 1A), confirming that PHR(-like) signaling as well as the
148 small AGPase subunit ADG1 are required for increased starch production under P_i starvation.
149 Concomitantly, P_i-depleted *adg1-1* mutants accumulated high levels of monosaccharides
150 (glucose and fructose, Figure 1A). Loss of TPT function caused significantly higher levels of
151 starch and glucose under P_i deprivation as compared to the WT, which resumed a trend that was
152 also observed under control conditions and likely reflects increased day-time starch turnover in
153 the *tpt-2* mutant (Schneider *et al.*, 2002). Interestingly, over-accumulation of carbohydrates by
154 *adg1-1* and *tpt-2* mutants under P_i deprivation was ceased in the double mutant *adg1 tpt-2*,
155 indicating that retrograde signaling of carbohydrate status is involved in this process. Likewise,
156 *adg1 tpt-2* double mutants failed to accumulate anthocyanins upon P_i deprivation (Supporting
157 Information Fig. S1A, B).

158 In order to test if nuclear gene regulation by PHR1/PHL1 is important for the adjustment
159 of P homeostasis when P_i recycling from photosynthetic intermediates is impaired, we
160 generated the triple mutant *adg1-1 phr1-3 phl1* (hereafter referred to as *adg1 phr1 phl1*). This
161 mutant exhibited a pronounced growth defect which was the result of reduced leaf size and
162 number (Figure 1B, C). Next, *adg1 phr1 phl1* plants flowered later than the parental lines
163 (Supporting Information Fig. S1C). These findings indicate that starch production functions
164 synergistically with PHR1/PHL1 in maintaining cellular P_i and/or carbohydrate homeostasis.

165 We noted that growth retardation of *adg1 phr1 phl1* resembled the phenotype of the
166 *adg1 tpt-2* mutant (Figure 1B). To test the hypothesis that *adg1 tpt-2* might likewise be affected
167 in P_i homeostasis, we measured P_i contents of aboveground tissues and determined P_i starvation
168 gene expression in vegetative plants grown on soil. Surprisingly, we found that *adg1 tpt-2*
169 double mutants over-accumulated P_i compared to the *adg1-1* single mutant (Figure 1D).

170 Counter-intuitively, quantitative RT-PCR (qRT-PCR) analysis revealed that transcripts of P_i
171 starvation marker genes including *SRG3*, *PS2*, *VPE1* (AT3G47420), *SPX1*, and *MGD3*
172 (Supporting Information Fig. S2) were all constitutively up-regulated in *adg1 tpt-2* (Figure 1E).
173 Additionally, transcript abundance of the circadian regulator *BASIC LEUCINE ZIPPER 63*
174 (*bZIP63*) (Baena-González *et al.*, 2007; Frank *et al.*, 2018), which is repressed by P_i depletion
175 in the WT (Supporting Information Fig. S2), was also reduced in rosettes of *adg1 tpt-2* as well
176 as *adg1-1* when grown on soil (Figure 1E). Interestingly, *tpt-2* on the contrary showed slightly
177 higher expression levels of *bZIP63* than WT plants. Thus, P_i signaling pathways are
178 substantially affected when triose phosphate utilization and allocation in the chloroplast are
179 compromised.

180 It was reported that the *adg1 tpt-2* mutant is sensitive towards higher light intensities,
181 which could be overcome by exogenously supplied sucrose (Schmitz *et al.*, 2012; Heinrichs *et*
182 *al.*, 2012). Given the phenotypic similarities between *adg1 tpt-2* and *adg1 phr1 phl1,* we asked
183 if the growth defect of *adg1 phr1 phl1* was also dependent on light intensity. In fact, we
184 observed high-light dependent growth restriction of *adg1 phr1 phl1* seedlings that was
185 comparable to *adg1 tpt-2*, both under low and high P_i conditions (Figure 1F; Supporting
186 Information Fig. S3). As for *adg1 tpt-2*, the difference in growth performance between low-
187 and high-light conditions was alleviated by providing sucrose to *adg1 phr1 phl1* mutants
188 (Figure 1F), a phenomenon that was also observed for root growth of the mutant seedlings
189 (Supporting Information Fig. S3). Remarkably, high-light dependent growth restriction was
190 also seen for both the *adg1-1* and *phr1-3 phl1* mutants, although to a lower extend than in the
191 cases of *adg1 tpt-2* and *adg1 phr1 phl1* (Figure 1F). Again, the difference in growth
192 performance between low and high light was attenuated by exogenous sucrose, indicating that
193 carbohydrate homeostasis is disturbed in *adg1-1*, *phr1-3 phl1*, and the triple mutant when
194 exposed to high light.

195 We concluded from these experiments that triose phosphate allocation has pronounced
196 effects on the nuclear P_i starvation response. Vice versa, P_i signaling is required for acclimation
197 to triose phosphate oversupply in high light or when starch production is genetically disabled.

198

199 **High light elicits P_i starvation gene expression in the WT**

200 The results of our reverse genetic analyses indicated that P_i homeostasis is affected by
201 photoassimilate availability and utilization. This raised the question whether P_i signaling was
202 also modulated in WT plants under non-starved conditions by naturally occurring changes in

203 the photosynthetic rate such as upon a shift in light intensity. In order to address this, we
204 interrogated published transcriptomic data collected from seedling shoots under P_i starvation
205 (Bustos *et al.*, 2010) and high-light treatments under nutrient-rich conditions (Huang *et al.*,
206 2019). We found that out of 379 transcripts upregulated ($\log_2$ fold change >2) by 30 min of high
207 light, 75 were also upregulated by P_i starvation (Figure 2A). For longer high-light treatments of
208 24 hours, 131 out of 564 transcripts were also P_i-responsive (Figure 2A). In both cases, the
209 overlap was found to be significant at $P < 0.0001$ in hypergeometric testing using Fisher's exact
210 test. In order to estimate whether the observed overlap between high-light and low-P_i induced
211 transcripts might be due to generally higher nutrient requirements under high-light conditions,
212 we next included a set of nitrogen-responsive transcripts in the comparison (Krapp *et al.*, 2011).
213 We detected a significant overlap of 33 transcripts that are differentially expressed in the shoots
214 under low nitrogen conditions with transcripts upregulated by a high-light treatment of 24 hours
215 duration (Figure 2A). In contrast, no significant enrichment of nitrogen-responsive transcripts
216 among high-light induced transcripts was observed for 30-min high-light treated plants (10 out
217 of 379). Thus, short-term high-light treatment specifically triggered low-P_i responses, while
218 long-term high-light stress seems to elevate general nutrient demand of the plant.

219 We next asked whether the induction of P_i-starvation responsive genes by short-term
220 high light required the activity of PHR1(-like) transcription factors and thus was truly caused
221 by low-P_i signaling pathways. To this end, we grew WT and *phr1-1 phl1* mutant plants under
222 nutrient-rich conditions on soil in an 8/16 hours (light/dark) photoregime. After 5 weeks, the
223 photon flux density was increased to 450±30 µmol m^{-2} s^{-1} (high light) at 1 hour after
224 commencement of the photoperiod, while the control group was kept under growth light
225 conditions of 70±5 µmol m^{-2} s^{-1}. We conducted qRT-PCR analysis of samples harvested after
226 20, 45, and 125 min of treatment and detected pronounced upregulation of *SRG3*, *SPX1*, and
227 *VPE1* transcripts in WT plants already after 20 min of exposure to high light compared to
228 control plants, as well as a slight increase in *MGD3* and *PS2* transcript abundance (Figure 2B).
229 In all five cases, the upregulation of gene expression was attenuated within 125 min in high
230 light, confirming that response to P_i shortage constitutes an early consequence of increased
231 irradiance. Crucially, P_i-starvation marker transcripts were not responsive to light conditions in
232 *phr1-1 phl1* mutant plants (Figure 2B), suggesting that PHR1/PHL1 are required for high-light
233 mediated regulation of these genes. Instead, we observed a tendency towards constitutively
234 higher transcript levels of most tested genes in the *phr1-1 phl1* mutants under control
235 conditions, particularly within the later timepoints of the analysis. This is likely caused by
236 activation of the remaining PHL genes in this mutant exhibiting chronically low P_i levels.

237 *PHR1* expression itself was reported to depend on light (Liu *et al.*, 2017). Importantly
238 however, increasing the light intensity to 450±30 µmol m^{-2} s^{-1} did not affect *PHR1* transcript
239 levels under our experimental conditions (Supporting Information Fig. S4), consistent with the
240 accumulation of *PHR1* transcript being only responsive to changes in the very low fluence range
241 (Liu *et al.*, 2017).

242 *GLUCOSE-6-PHOSPHATE/PHOSPHATE TRANSLOCATOR 2* (*GPT2*) is a light
243 responsive gene (Athanasiou *et al.*, 2010) which was also described to be induced by P_i
244 starvation (Morcuende *et al.*, 2007). Furthermore, high-light induced expression of *GPT2* was
245 previously described to depend on *TPT* function (Kunz *et al.*, 2010; Weise *et al.*, 2019), and we
246 noted that the promotor sequence of *GPT2* contains a PHR1 binding motif (GTATATTC) close
247 to the transcriptional start site. However, in our high-light experiment, *GPT2* was upregulated
248 in both WT and *phr1-1 phl1* after 45 minutes, and transcript levels continued to rise upon stress
249 during the course of the analysis (Figure 2B). This showed that PHR1/PHL1 are not required
250 for high-light mediated induction of *GPT2* expression. Moreover, we were not able to detect an
251 effect of the *gpt2-1* allele (Niewiadomski *et al.*, 2005) on carbohydrate accumulation under P_i
252 depletion (Supporting Information Fig. S5), arguing against a major role of this gene for sugar
253 homeostasis under P_i starvation. Thus, *GPT2* induction under high light is independent of
254 PHR1(-like) signaling, and *phr1 phl1* mutants are not generally impaired in the transcriptional
255 response to high light. Nevertheless, high-light treatment at early timepoints specifically
256 triggers low-P_i signaling resulting in the upregulation of transcripts such as *SRG3*, *SPX1*, and
257 *VPE1*.

258

259 **Short-term high light affects chloroplast P_i levels and sucrose accumulation**

260 Upregulation of P_i starvation marker genes upon short-term high light suggested the
261 existence of a light-induced signal resulting in the activation of PHR1(-like) transcription
262 factors. Since PHR1(-like) activity is primarily regulated by the P_i status of the cell, we asked
263 whether cellular P_i reserves were affected by high light, thus relieving PHR(-like) transcription
264 factors of SPX-mediated inhibition. To address this, we performed non-aqueous fractionation
265 of plant rosettes subjected to high light for 20 min or kept under control conditions, and
266 determined subcellular concentrations of free P_i. Under control conditions, WT and *phr1-1 phl1*
267 mutant plants clearly differed in vacuolar P_i reserves (14 % of WT level in *phr1-1 phl1*),
268 chloroplast P_i content (50 %), as well as the cytosolic and nuclear P_i fraction (63 %) (Figure
269 3A). Strikingly, high-light treatment caused a decline in chloroplast P_i levels by 54 % in the

270 WT (Figure 3A), decreasing to 0.4 µmol P_i g^{-1} dry weight which corresponds to a concentration
271 of about 0.12 mM P_i (Santarius & Heber, 1965). Consequently, P_i levels of high-light treated
272 chloroplasts in the WT approximated the P_i levels measured in chloroplasts of *phr1-1 phl1*
273 under control conditions. In contrast, no light-dependent effect was seen for P_i levels in the
274 double mutant. Importantly, P_i concentrations of the cytosolic/nuclear and vacuolar fractions
275 were not significantly altered by high light in either WT or *phr1-1 phl1* mutant plants (Figure
276 3A). Hence, elevated light rapidly induced P_i depletion in the WT, however the effect remained
277 restricted to the chloroplast, and therefore does not qualify as a direct cause of PHR1/PHL1
278 activation upon high light.

279 PHR1(-like) regulation by inositol pyrophosphates relates to the metabolism of these signaling
280 compounds in the cytosol (Wild *et al.*, 2016) which depends on both P_i and ATP levels (Zhu *et*
281 *al.*, 2019; Riemer *et al.*, 2021). Given that cytosolic P_i concentrations were unchanged by 20
282 min high-light treatments, we asked if light increase affected cellular ATP levels. While
283 *phr1-1 phl1* double mutants exhibited a tendency towards lover ATP levels that was more
284 pronounced upon high-light treatment, light increase did not significantly affect ATP or ADP
285 levels in the WT at 20 or 90 min of treatment (Figure 3B). Hence, activation of PHR1(-like)
286 transcription by short-term high light appears to be independent of cytosolic P_i and ATP levels.

287 It has been reported that P_i starvation responses are modulated by sugar availability (Franco-
288 Zorrilla *et al.*, 2005; Müller *et al.*, 2005, 2007; Karthikeyan *et al.*, 2007). Since sugars are also
289 involved in the signaling of photosynthetic status (Häusler *et al.*, 2014; Li & Sheen, 2016;
290 Zirngibl *et al.*, 2023), we tested if short-term high-light treatment was sufficient to induce
291 changes in sugar levels in leaves. At the timepoint tested, i.e. 80 min after onset of the
292 photoperiod, contents of sucrose under control conditions were found to be lower in leaves of
293 *phr1-1 phl1* as compared to the WT (Figure 3C). 20 min high-light treatment resulted in a
294 further increase in sucrose (Figure 3C), but not glucose or fructose (Supporting Information
295 Fig. S6) levels in the WT. A similar fold-change of sucrose contents was observed in
296 *phr1-1 phl1* mutant leaves upon high light, although the increase in absolute levels was not
297 significant (Figure 3C). Thus, sucrose levels respond to high-light treatment on a very short
298 timescale, suggesting that they might act as early signaling compounds, and potentially might
299 also affect light-dependent P_i starvation responses.

300 Analysis of transcriptomic data revealed upregulation of both P_i and nitrogen starvation
301 responses upon medium-term (24 h) high light (Figure 2A). To address if this was attributable
302 to enhanced nutrient requirements caused by high light, we determined total P_i contents of

303 rosettes subjected to 24 and 48 h of light increase. In fact, shoot P_i levels of WT plants were
304 slightly reduced within 48 h of high light as compared to control light conditions (Figure 3D).
305 This correlated with significantly enhanced plant biomass measured upon 48 h of high light
306 compared to control treatments (Figure 3D), suggesting that light increase stimulated growth
307 which was not immediately satisfied by additional nutrient acquisition. In contrast to WT plants,
308 P_i contents in leaves of *phr1-1 phl1* mutant plants remained at low levels independently of the
309 light treatment (Figure 3D).

310 Together, our results indicate that induction of P_i starvation responses upon light increase
311 occurs in at least two phases: Short-term (20-45 min) responses are triggered by a signal
312 independent of cytosolic/nuclear P_i concentrations. This short-term signal communicates
313 chloroplast P_i levels to the nucleus, and/or potentially involves cellular sucrose levels. In the
314 medium term however, a shift to higher light intensities causes cellular P_i depletion through an
315 imbalance of growth and nutrient uptake.

316

317 **Carbohydrate accumulation is affected in *phr1 phl1* mutants**

318 We asked if the induction of P_i starvation gene expression was relevant for the
319 acclimation of photosynthetic processes to increased radiation. To this end, we first performed
320 pulse-amplitude modulated (PAM) chlorophyll fluorometry on rosette leaves subjected to
321 increased light. The efficiency of photosystem II photochemistry (ΦPSII) dropped to the same
322 extent in both WT and *phr1-1 phl1* mutants upon exposure to increased illumination for
323 125 min (Figure 4A). After 125 min of treatment, also the maximum efficiency of PSII (F_v/F_m)
324 had decreased significantly in the stressed plants of both genotypes (Figure 4B). As for ΦPSII,
325 no difference was observed for F_v/F_m between WT and *phr1-1 phl1*, indicating that thylakoid
326 reactions were not affected in *phr1-1 phl1* mutants.

327 Next, we determined the changes in carbohydrate contents that occurred within 90 min
328 upon an increase in photon flux density from 70±5 µmol m^{-2} s^{-1} to 450±30 µmol m^{-2} s^{-1} in
329 rosette leaves of 5-weeks-old WT and *phr1-1 phl1* mutant plants. As shown in Figure 4C, starch
330 contents under control conditions were higher in *phr1-1 phl1* mutants than in the WT. This may
331 be related to the fact that *phr1-1 phl1* mutants manifest lower P_i levels in the chloroplasts
332 (Figure 3A), a condition that allosterically activates AGPase (Figueroa *et al.*, 2022). High-light
333 treatment caused an increase in starch contents in both WT and mutant (Figure 4C). However,
334 the fold change of starch content upon high light was lower in *phr1-1 phl1* than in WT plants.
335 This was accompanied by slightly lower levels of monosaccharides (glucose and fructose), but

336 not sucrose, in the double mutant upon 90 min of light increase (Figure 4E). Notably,
337 differences in sucrose levels that were seen between WT and *phr1-1 phl1* under control growth
338 at 80 min after the onset of the photoperiod (Figure 3C), were not detected at 150 min into the
339 photoperiod (Figure 4E), indicating that sucrose levels are disturbed in *phr1-1 phl1* during the
340 early morning.

341 In conclusion, carbon fixation and/or allocation is slightly compromised in *phr1-1 phl1*
342 mutants upon high light, while WT-like sucrose levels are maintained during the later course
343 of the day, independent of light conditions.

344

345 **PHR1/PHL1 are involved in high-light-mediated anthocyanin accumulation**

346 Since both P_i starvation and high-light stress trigger anthocyanin production, we next
347 analyzed the role of *PHR1/PHL1* signaling in anthocyanin accumulation during high-light
348 acclimation. As shown in Figure 4D, anthocyanin contents of *phr1 phl1* leaves after 3 days of
349 high-light exposure were significantly lower than in WT leaves or in the single mutants *phr1-3*
350 and *phl1*, while loss of *SPX1/2* function did not have any statistically significant effect. PHR1
351 has been implicated in flavonoid biosynthetic gene induction under low P_i (He *et al.*, 2021; Liu
352 *et al.*, 2022). We did not detect significant differences in the induction of *LDOX*, *DFR*, *PAP1*,
353 or *MYB111* transcripts between WT and *phr1-1 phl1* mutants at 24 or 48 h of light increase
354 (Supporting Information Fig. S7). Interestingly however, *PAP2* expression was markedly
355 upregulated in *phr1-1 phl1* compared to the WT at 24 h of high light (Supporting Information
356 Fig. S7), indicating that the regulation of anthocyanin accumulation is disturbed at a different
357 level than biosynthetic gene expression in *phr1-1 phl1*.

358 It has been reported that high-light induced anthocyanin biosynthesis depends on
359 sucrose signaling (Zirngibl *et al.*, 2023). Given that sucrose levels were similar between WT
360 and *phr1-1 phl1* at 90 min of high light (Figure 4E), we reasoned that sugar-mediated
361 anthocyanin production might be impaired at the signaling level in *phr1-1 phl1*. To address this,
362 we exposed 7-days old seedlings grown on nutrient-rich media to sucrose- or sorbitol-
363 containing media with different P_i supplies for 67 hours. As depicted in Figure 4F, 3 days of
364 mere P_i depletion were not sufficient to trigger measurable anthocyanin production in either
365 genotype. When sorbitol was added to the media, WT and *phr1-1 phl1* seedlings accumulated
366 anthocyanins to the same level (Figure 4F), indicating that WT and *phr1-1 phl1* are
367 indistinguishable in terms of anthocyanin production upon osmotic stress. Crucially, when
368 sorbitol containing media were compared to media containing sucrose at same-osmotic effect

369 concentrations, *phr1-1 phl1* mutants failed to produce anthocyanins above the level of the
370 osmotic effect when the growth medium lacked P_i (Figure 4F). Thus, *phr1-1 phl1* mutants are
371 specifically defective in sucrose-mediated anthocyanin production already at early stages of P_i
372 depletion.

373 Taken together, *PHR1/PHL1* functions are required for adequate high-light mediated
374 anthocyanin accumulation, which might be related to a role in sucrose signaling upon cellular
375 P_i restriction.

376

377 **_SRG3_ expression is required for lipid homeostasis upon light increase**

378 Among the *PHR1/PHL1*-dependent transcripts analyzed under short-term high light,
379 *SRG3* showed particularly strong upregulation (Figure 2B), and it has been suggested that the
380 *SRG3* promoter is directly activated by PHR1 (Cheng *et al.*, 2011). To test this hypothesis, we
381 performed promoter-transactivation assays in mesophyll protoplasts. PHR1 was able to induce
382 the expression of a luciferase reporter fused to the promoters of *SRG3*, *MGD3*, *GPT2*, and *SPX1*
383 (lacking the naturally occurring *Nco*I restriction site, $proSPX1^{GC}$) (Figure 5A). Notably
384 however, the responsiveness of *proGPT2* to *PHR1* expression was considerably lower than
385 observed with the constructs harboring $proSPX1^{GC}$, *proSRG3* or *proMGD3* upstream of the
386 reporter CDS. This finding was consistent with the observation that *GPT2* was induced
387 independently of *PHR1/PHL1* under high light (Figure 2B), and suggests that *SRG3*, like
388 *MGD3* and *SPX1*, is a veritable target gene of PHR1.

389 We next asked whether PHR1-mediated induction of *SRG3* was relevant for lipid
390 metabolism upon light increase, given the proposed role of SRG3 in phospholipid degradation
391 pathways. To answer the question, we compared the lipid profile of a four-week-old WT and
392 *srg3* loss-of-function mutant (Cheng et al., 2011) grown in soil, which had been exposed to
393 high light for two or seven hours. The two-hour exposure was an early timepoint of acclimation,
394 close to the onset of gene expression, while the seven-hour exposure corresponded to the end
395 of the light period to allow for a stronger metabolic response. Total lipid extracts of shock-
396 frozen leaf material were analyzed by ultra-performance liquid chromatography coupled to a
397 quadrupole time-of-flight mass spectrometer equipped with electrospray ionization source. The
398 first principal component of the PCA analysis (Figure 5B) on the aligned 2478 lipid features
399 (Supporting Information Table S1) accounted for 50 % of the total variance, suggesting
400 differences in the lipidome of *srg3* compared to the WT. Therefore, we profiled the main
401 structural lipids monogalactosyl diacylglycerols (MGDG), digalactosyl diacylglycerols

402 (DGDG), sulfoquinovosyl diacylglycerols (SQDG), phosphatidylcholines (PC),
403 phosphatidylglycerols (PG) and phosphatidylinositols (PI) in WT and *srg3* after 2 h and 7 h of
404 light stress. Their total levels were comparable (Supporting Information Fig. S8A), which is
405 consistent with the results obtained for *srg3* mutants under P_i starvation conditions (Cheng *et*
406 *al.*, 2011). Notably, the levels of MGDG(34:1), DGDG(34:1) and DGDG(34:2) were slightly
407 higher in both WT and *srg3* after 7 h of high light (Supporting Information Fig. S9), whereas
408 the levels of the phospholipids determined were comparable (Supporting Information Fig. S10).
409 In addition, profiling of sphingolipids revealed non-significant higher levels of ceramides in
410 *srg3* compared to WT in all four investigated conditions, but hydroxy ceramides and glucosyl
411 ceramides were WT-like in the mutant (Supporting Information Fig. S8B).

412 We also performed lipid profiling of acyl-MGDGs and Arabidopsides in the extracts,
413 as galactolipids can be acylated or oxygenated (Ibrahim *et al.*, 2011). We could only identify
414 acyl-MGDG-54:8 and Arabidopside A (1-OPDA, 2-dnOPDA MGDG), and their levels were
415 significantly higher in *srg3* after 7 h of high light stress compared to the other groups (Figure
416 5C). This result encouraged us to perform ANOVA on the annotated 2478 lipid features
417 (Supporting Information Table S2) in order to identify more *srg3*-dependent high-light
418 responsive lipids. We first selected lipid features that were significantly different between WT
419 plants treated with 7 h of high light and untreated plants. ANOVA revealed 81 lipid features
420 (fold change ≥ 2, $P \leq 0.05$) whose intensities were different after exposure to high light for 7 h
421 (Supporting Information Table S2). Of the 81 lipid features that respond to high light in the
422 WT, 18 were significantly different in *srg3* compared to WT after 7 h of high light (Supporting
423 Information Table S3). One of them was identified as linolenic acid, whose levels were higher
424 in *srg3* compared to WT after 7 h but not 2 h of high light (Figure 5C), like Arabidopside A
425 and MGDG-54:8. Interestingly, a lipid feature was constitutively higher in *srg3* and
426 accumulated upon high-light treatment (Figure 5C), which we could tentatively assign to a
427 glycosylated SQDG species (SQDG-34:1+$C_5H_8O_4$; Supporting Information Table S3). The
428 identification of this unknown lipid species will need to be verified in the future using tandem
429 mass spectrometry and nuclear magnetic resonance spectrophotometry after purification.

430 One of the *srg3*-dependent metabolite features showing highest light-responsiveness
431 was identified as zeaxanthin (Figure 5C; Supporting Information Table S3), a photoprotective
432 carotenoid and component of the xanthophyll cycle (Demmig-Adams & Adams, 1996; Havaux
433 & Niyogi, 1999). In *srg3*, zeaxanthin accumulation following 7 h of high light was reduced by
434 one third as compared to the WT, indicative of a reduced capacity for light energy dissipation
435 in chloroplast membranes of *srg3*. To further investigate this, we performed PAM chlorophyll

436 fluorescence measurements and determined the light response of the non-photochemical
437 quenching (NPQ) parameter in WT, *srg3*, and *phr1-1 phl1* mutant plants. Indeed, the extend of
438 NPQ was slightly but significantly reduced in both the *srg3* and the *phr1-1 phl1* mutants
439 compared to the WT (Figure 5F). Taken together, *SRG3* expression is required for maintaining
440 fatty acid homeostasis and the establishment of light protection upon high-light stress.

441

442 ***SRG3* contributes to triacylglycerol accumulation upon light increase**

443 The observation that linolenic acid accumulated in *srg3* leaves upon high light (Figure
444 5C) raised the question as to whether containment of free fatty acids was impaired by *srg3*
445 mutation. One strategy to reduce the levels of cytotoxic fatty acids in plant cells is their
446 incorporation into triacylglycerols (TAG) under stress, including P_i starvation (Pant *et al.*, 2015;
447 Yang & Benning, 2018). We therefore quantified total TAG levels and found a pronounced
448 accumulation after 7 h of light treatment in the wildtype (Figure 5D). In *srg3* mutants, high-
449 light induced TAG accumulation was significantly lower. The differences between WT and
450 mutant were due to reduced accumulation of TAG species with long-chain fatty acids exhibiting
451 higher degree of desaturation (54:6, 54:7, 54:8, 54:9) in *srg3* (Supporting Information Fig. S12),
452 which would be accordant with linolenic acid esterification. TAG species with polyunsaturated
453 54-carbon acyl chains also showed the highest changes in the WT upon high light (Figure 5E),
454 a pattern that is reminiscent of heat-stress induced TAG accumulation (Mueller *et al.*, 2015).
455 To control if high light caused a heat response in the treated plants, we analyzed transcript levels
456 of *HEAT SHOCK PROTEIN 70* (*HSP70*) and *HSP18.2*, previously used to discriminate light
457 and heat responses (Huang *et al.*, 2019). High light under our experimental conditions caused
458 accumulation of *HSP70* and, to a lesser extent, *HSP18.2* transcripts which was mostly confined
459 to the 45 min timepoint of treatment (Supporting Information Fig. S13). While *HSP70* induction
460 upon high light was also seen by Huang *et al.* (2019), *HSP18.2* transcript accumulation is
461 indicative of a mild heat response under the conditions used in this study. Thus, we cannot fully
462 exclude that TAG accumulation observed upon high-light treatments was triggered by higher
463 temperature at the leaf surface. Nevertheless, the late appearance of TAG enrichment after 7
464 hours of high-light treatment, as opposed to the moderate and transient induction of *HSP18.2*
465 at 45 min of treatment, suggests that the observed changes might indeed be triggered by high-
466 light treatment independently of temperature effects. Our analysis of TAG accumulation in *srg3*
467 mutant plants furthermore suggest that *SRG3* gene function is required for normal occurrence
468 of stress-induced TAG enrichment.

469 # Discussion

470 P_i is intimately linked to photosynthetic metabolism, both as a substrate for
471 photophosphorylation, and as a potent kinetic regulator of carbon assimilation (Furbank &
472 Lilley, 1980; Stitt *et al.*, 1983; Preiss, 1984; Hendriks *et al.*, 2003; Marcus *et al.*, 2005).
473 Additionally, P_i starvation responses affect the photosynthetic machinery of plants (Giersch &
474 Robinson, 1987; Fredeen *et al.*, 1990; Liu *et al.*, 2024) which is partially achieved at the
475 transcriptional level (Wu *et al.*, 2003; Morcuende *et al.*, 2007; Bustos *et al.*, 2010; Nilsson *et*
476 *al.*, 2012). Nevertheless, it has remained elusive whether changes in the metabolic P_i demand
477 of the chloroplast relay to the nuclear P_i starvation response. The observations presented herein
478 establish that the P_i response machinery involving the transcription factors PHR1 and PHL1 is
479 activated by an increase in photosynthetic activity, and we provide evidence that *PHR1/PHL1*
480 contribute to the rapid metabolic adjustment during changes in light intensity (Figure 6).

481

482 **Increase in light intensity creates a transient low-P_i signal**

483 Transcriptional responses to changes in light intensity can be observed on the timescale
484 of minutes (Vogel *et al.*, 2014; Huang *et al.*, 2019), but the signaling cascades behind are
485 incompletely elucidated. We noted that the transcriptomic changes upon a shift to high light
486 overlap with those observed during growth under P_i-limited conditions (Figure 2A).
487 Interestingly, a previous study addressing intraspecies variation of the transcriptional response
488 to increased irradiance recognized the induction of P_i-starvation responsive genes upon high
489 light in two out of three tested accessions of Arabidopsis, and PHR1-target gene induction
490 coincided with photosynthetic efficiency of the ecotypes (van Rooijen *et al.*, 2018). Among the
491 high-light and low-P_i induced transcripts, we quantified the expression of *SRG3*, *SPX1*, and
492 *VPE1* during the early phase of high-light acclimation and determined that these transcripts
493 transiently accumulate already at 20 min of exposure to increased photon flux density (Figure
494 2B). Crucially, gene induction was absent in *phr1-1 phl1* double mutants, qualifying this short-
495 term high-light response as dependent on nuclear low-P_i signaling. Hence, plant cells are
496 capable of exploiting the transcriptional potential of the low-P_i response module in order to
497 react to environmental stimuli, even under nutrient-replenished conditions. Notably, high-light
498 mediated induction was not seen to the same extend for all PHR1 targets examined, as
499 expression of *MGD3* and *PS2* were only marginal (Figure 2B). This suggests that short-term
500 high light affects only a subset of the transcriptional P_i starvation response, potentially
501 reflecting differential chromatin accessibility of the genes (Barragán-Rosillo *et al.*, 2021).

502 How are PHR1 and PHL1 activated by an increase in light intensity? It has been
503 established that photosynthetic activity, through the production of phosphorylated assimilates,
504 reduces the P_i pool available for photophosphorylation (Sharkey, 1985; Walker & Sivak, 1986;
505 Robinson & Giersch, 1987; McClain & Sharkey, 2019), but the effect on other cellular
506 compartments than the chloroplast has remained obscure. Our analysis of subcellular P_i contents
507 revealed a reduction of chloroplast P_i by more than one half upon an increase in light intensity
508 of 20 min duration (Figure 3A). Meanwhile, no decline in the cytosolic/nuclear or the vacuolar
509 fractions was observed, proving high capacity of the cell to control subcellular P_i distribution.
510 This finding however argues against InsP8-dependent PHR1(-like) activation under these
511 conditions. Given the large difference in vacuolar P_i levels compared to the cytoplasm, we
512 cannot fully rule out that a difference in the P_i levels between treated and control cytosolic
513 preparations was masked by minor vacuolar contaminations. It is also possible that a drop in
514 cytosolic P_i levels sufficient to trigger a peak in PHR1(-like) activity occurs transiently prior to
515 the sampling timepoint and therefore precedes transcript accumulation seen at 20 min of
516 treatment. However, our finding is consistent with the assumption that P_i exchange between
517 chloroplast and cytosol (Santarius & Heber, 1965), and even more so between cytosol and
518 vacuole (Woodrow *et al.*, 1984) are rather slow processes. Additionally, the rapid increase in
519 sucrose levels that can be observed upon high light (Figure 3C) indicates that the capacity for
520 P_i liberation via sucrose biosynthesis might be sufficient to balance cytosolic P_i levels against
521 depletion through triose phosphate import.

522 Intriguingly, our observations would be coherent with the possibility that P_i levels of
523 the chloroplast are directly sensed to promote PHR1(-like) activation upon high light. Evidence
524 for a role of chloroplast P_i levels in the acclimation of the photosynthetic machinery was
525 recently provided by Raju et al. (2024) who investigated stromal P_i levels of mutants defective
526 in P_i transporters of the chloroplast envelope using a FRET-based P_i sensor. Here, P_i levels in
527 the stroma of *tpt*, *pht2;1*, and double mutants correlated with ΦPSII and NPQ parameters, while
528 proton motif force and proton efflux efficiency of the ATP synthase, as determined by
529 electrochromic shift measurements, were not affected after 2 min of a dark-light transition. The
530 latter finding is corroborated by our result that ATP levels of WT plants are unaffected upon
531 light increase, although ATP synthesis in the chloroplast would be expected to be kinetically
532 constrained at the P_i concentrations measured in our system (Sharkey, 1985; McClain &
533 Sharkey, 2019). Chloroplast P_i acting as an original retrograde signal would serve as an
534 explanation for high constitutive PHR1(-like) activation in the *adg1 tpt-2* mutant (Figure 1E).
535 Here, metabolically available P_i levels are likely very low given that the mutant is defective in

536 major pathways of triose phosphate utilization. Hence, bulk release of P_i in *adg1 tpt-2* might be
537 restricted to glycolysis and vacuolar phosphatase activity acting on phosphorylated organic
538 compounds such as phosphoenolpyruvate (Ohnishi *et al.*, 2018). This would cause unequal
539 intracellular pool sizes of free P_i, characterized by high vacuolar P_i stores (Figure 1D), and
540 particularly low P_i levels in the chloroplast. It will be insightful to examine the subcellular
541 distribution of P_i in the *adg1 tpt-2* mutant during future studies in order to elucidate the function
542 of chloroplast P_i in retrograde signaling, and in the pleiotropic phenotypes of the *adg1 tpt-2*
543 mutant.

544

545 **PHR1/PHL1 act in the network of sugar signaling**

546 Blocking starch production in the *phr1-3 phl1* double mutant by introduction of the
547 *adg1-1* allele substantially restricted growth (Figure 1B, C, F). In line with this, *phr1-1 phl1*
548 mutants over-accumulated starch at the adult stage (Figure 4C), indicating that starch
549 biosynthesis aids metabolism when cellular P_i levels are chronically depleted as it is observed
550 in *phr1 phl1* mutants (Figure 3A, D). In fact, it is estimated that the bulk of P sequestered in
551 photoassimilates is liberated via starch and sucrose biosynthesis (McClain & Sharkey, 2019).
552 In line with the assumption that chloroplast P_i reserves are exploited through photosynthetic P_i
553 consumption, growth restriction of *phr1-3 phl1*, *adg1-1*, and particularly *adg1 phr1 phl1*
554 seedlings was more pronounced under high-light growth conditions (Figure 1F). However
555 counter-intuitively, this was alleviated by an additional carbohydrate source supplied via the
556 growth medium (Figure 1F), suggesting that metabolic alterations in these mutants extend
557 beyond an insufficient capacity for P_i recycling for photoassimilation. It has been concluded
558 from the studies on *adg1 tpt-2* mutants that sugars act as retrograde signaling molecules
559 communicating photosynthetic status to the nuclear genome (Heinrichs *et al.*, 2012; Häusler *et*
560 *al.*, 2014; Schmitz *et al.*, 2014). Like in *adg1 tpt-2* (Schmitz *et al.*, 2014), acclimation to high-
561 light growth conditions might be impaired in *adg1 phr1 phl1*, and to a lesser extend in *phr1 phl1*
562 mutants, resulting from a depletion of carbohydrates that occurs in the long-term of light
563 exposure. In fact, already under the moderate growth light conditions, we noted time-of-day
564 dependent deficits in sucrose levels in adult *phr1-1 phl1* plants (Figure 3C, 4E), similar to
565 *adg1 tpt-2* mutants that lack diurnal peaks in sucrose concentrations (Schmitz *et al.*, 2012).
566 Moreover, *phr1 phl1* mutants exhibit a phenotype of early leaf senescence (Bustos *et al.*, 2010;
567 Wang *et al.*, 2023) that is reminiscent of the symptoms caused by carbohydrate depletion.
568 Interestingly, Schmitz et al. (2014) also noted that *adg1-1* mutation was associated with

569 transcriptomic changes affecting lipid metabolism as we report here for the *PHR1/PHL1*-
570 mediated high-light response. Finally, *phr1 phl1* mutants were specifically insensitive towards
571 sucrose in terms of anthocyanin production under early P_i-depleted growth conditions (Figure
572 4F). We therefore propose a function of PHR1/PHL1 in sugar signaling, thus contributing to
573 the adjustment of the C/P balance.

574

575 **PHR1/PHL1 promote acclimation to higher light intensities**

576 Our analysis of the *PHR1/PHL1* dependent transcriptional response to high light
577 focused on *SRG3*, *SPX1*, and *VPE1*. *VPE1* induction, putatively encoding a vacuolar efflux
578 transporter (Xu *et al.*, 2019), immediately suggests itself as a strategy for intracellular P_i
579 redistribution in favor of the cytosol by exploitation of the vacuolar P_i stores. This would serve
580 to provide additional P_i to metabolic pathways, which seems adequate since light increase
581 represents a condition that accelerates growth rate and implies higher nutrient demand in the
582 mid-term (Figure 3D). In contrast, *SPX1* as a highly responsive P_i starvation marker gene (Wang
583 *et al.*, 2023) functions in negative feed-back of P_i starvation responses (Puga *et al.*, 2014). Such
584 fine-tuning of PHR1(-like) activation under light increase seems appropriate given the
585 fluctuating nature of this environmental factor.

586 The pronounced PHR1/PHL1 dependent induction of *SRG3* was further investigated
587 within this study. The mechanistic contribution of SRG3 to P_i homeostasis is indistinct, and it
588 has been reported in other plant species that GDPD isoforms play a role in phospholipid
589 homeostasis (Dang *et al.*, 2025), but also in hormone signaling and the modulation of root
590 morphology upon P_i starvation (Mai *et al.*, 2021; Hu *et al.*, 2024; Verma *et al.*, 2025). We
591 demonstrated here that the *SRG3* promotor is activated by over-expression of *PHR1* in
592 mesophyll protoplasts (Figure 5A), indicating that it constitutes a true target of the transcription
593 factor. To elucidate a potential physiological function of *SRG3* expression for lipid metabolism
594 in the light acclimation response of shoots, we set out to identify lipid features that were altered
595 by *srg3* mutation upon high-light treatment using an untargeted approach. Comparing WT and
596 *srg3* rosette leaves, we detected differences in the lipid fingerprints particularly after longer
597 treatment duration (Figure 5B). Among the molecules that over-accumulated in *srg3* mutants
598 in a high-light dependent manner, we identified linolenic acid, the galactolipid derivatives acyl-
599 MGDG (54:8), and Arabidopside A, as well as a molecule that was constitutively upregulated
600 in *srg3* and putatively represents glucosylated SQDG (Figure 5C). While the latter lipid species
601 has to our knowledge not been reported before, accumulation of the remaining species draws

602 the picture that *srg3* mutants experience stress during acclimation to higher light intensities.
603 Both acyl-MGDG and Arabidopside accumulation have been reported to be associated with
604 stress conditions (Buseman *et al.*, 2006; Vu *et al.*, 2014; Nilsson *et al.*, 2016), and it was
605 suggested that the pool of acyl-MGDG increases upon stress to sequester oxidized fatty acids
606 (Vu *et al.*, 2014). Moreover, Arabidopside A has been ascribed a role in the regulation of
607 chlorophyll degradation during senescence processes (Weber, 2002; Hisamatsu *et al.*, 2006).
608 Thus, the lipid fingerprint of *srg3* upon light increase implies that the gene might be required
609 to maintain the integrity of photosynthetic membrane components upon changes in light
610 availability. The accumulation of linolenic acid in leaves of light-stressed *srg3* plants
611 furthermore indicates that the processing of fatty acids is disturbed in the mutant. After 7 h of
612 high light, we observed an increase in galactolipid species with low degree of desaturation in
613 WT and mutant plants (Supporting Information Fig. S9), an aspect of short-term high-light
614 acclimation that has been reported before (Burgos *et al.*, 2011). Such membrane remodeling
615 involves lipid degradation and can be assumed to generate free fatty acids with higher degree
616 of desaturation, including linolenic acid. Hence, SRG3 might fulfill a function in the
617 containment of such products derived from membrane remodeling. The product of SRG3
618 activity, glycerol-3-phosphate (Cheng *et al.*, 2011), is a substrate for membrane lipid
619 biosynthesis, as well as for TAG production (Bates, 2016), both of which also require fatty acid
620 precursors. To test whether any of these pathways is constrained in *srg3*, giving rise to higher
621 linolenic acid levels, we quantified the pools of predominant membrane lipids and TAGs. While
622 the levels of major lipid classes were unaffected by *srg3* mutation (Supporting Information Fig.
623 S8), we detected TAG accumulation in the WT after 7 h of light increase which was slightly
624 reduced in *srg3* mutants (Figure 5C). Consistent with a potential involvement of SRG3 in
625 plastoglobule formation, TAG profiles revealed that the species with strongest accumulation
626 under our high-light conditions also contained linolenic acid (Figure 5E, Supporting
627 Information Fig. S12). Notably, linolenic acid is also a component of the acyl-MGDG (54:8)
628 species which was enriched in *srg3* upon high light, confirming high availability of this fatty
629 acid in *srg3* under stress. Elevated levels of free fatty acids can be cytotoxic probably due to
630 their amphipathic and detergent-like properties leading to the inhibition of photosynthesis and
631 damage to PSII (Kunz *et al.*, 2009). Thus, our results suggest that SRG3 contributes to the
632 detoxification of free linolenic acid that is released during high light-induced membrane
633 remodeling by incorporation of excess linolenic acid into TAGs. Notably, linolenic acid
634 accumulation was previously also observed in Arabidopsis plants subjected to salinity stress,
635 and this was connected to the control of ion homeostasis via the regulation of H^+-ATPase

activity (Han *et al.*, 2017; Abdelrahman *et al.*, 2021). Hence, instead of a direct involvement of SRG3 in the processing of fatty acids, linolenic acid accumulation in *srg3* might also be a secondary effect related to perturbed membrane remodeling.

Interestingly, a compound that accumulated upon light increase in the WT, but was reduced by *srg3* mutation, was identified as zeaxanthin (Figure 5C), a molecule that is involved in the protection against excess excitation energy as part of the xanthophyll cycle (Demmig-Adams & Adams, 1996; Havaux & Niyogi, 1999; Sacharz *et al.*, 2017). In line with a function of both *SRG3* and *PHR1*/*PHL1* for proper operation of the xanthophyll cycle, assessment of the NPQ component of chlorophyll a fluorescence revealed deficits in both mutant genotypes (Figure 5F). It is well-known that the membrane lipid composition is important for the xanthophyll cycle, and both lipid class and fatty acid composition determine faithful operation of all components (Goss & Latowski, 2020). Hence, it is tempting to hypothesize that *SRG3* expression, induced by the nuclear low-P_i response machinery, might be required for the adjustment of the membrane environment to ensure proper function of the enzymes involved in the xanthophyll cycle. Strikingly, this might be directly related to the changes in chloroplast P_i levels seen under high light (Figure 3A), given the recent observations on NPQ levels of P_i-transport mutants made by Raju et al. (2024) which were mentioned above. We therefore propose a signaling pathway originating from photosynthetic activity that engages PHR1 and PHL1 to induce *SRG3* expression for the acclimation of the photosynthetic membranes towards high light.

Conclusions

High-light stress requires immediate responses to avert damage to cellular components. As a new mode of signaling excess photosynthetic activity, we describe a function of the low-P_i response machinery involving PHR1 and PHL1 transcription factors under nutrient replete growth conditions. Our results indicate that chloroplast P_i sequestration into phosphorylated photoassimilates, and/or the accumulation of these photoassimilates, create a retrograde signal resulting in the activation of PHR1 and PHL1 in the cytosol and nucleus. This serves to mobilize cellular P_i, and to support acclimation responses including anthocyanin production, and the adjustment of lipid metabolism to ensure photoprotection and fatty acid homeostasis.

667 # Materials and Methods

668 **Plant material**

669 All Arabidopsis plants used in this study are in the background of the Columbia-0
670 accession. The *phr1-3* (AT4G28610; SALK_067629C) (Nilsson *et al.*, 2007) and *phl1*
671 (AT5G29000; SAIL_731_B09) (Klecker *et al.*, 2014) lines were described previously and the
672 derived homozygous double mutant *phr1-3 phl1* was a kind gift of Angelika Mustroph
673 (University of Bayreuth). The double mutant *phr1-1 phl1* (Bustos *et al.*, 2010) was backcrossed
674 to *phl1* in order to remove a transgene containing the *NPTII* cassette which was previously
675 introduced for isolation of the *phr1-1* allele (Rubio *et al.*, 2001). All experiments were
676 performed with the homozygous double mutant *phr1-1 phl1* lacking the *NPTII* cassette. The
677 double mutant *spx1 spx2* was described earlier (Puga *et al.*, 2014). Knockout lines *adg1-1*
678 (At5g48300) (Lin *et al.*, 1988), *tpt-2* (At5g46110; SALK_073707.54.25.x) and *adg1 tpt-2*
679 (Schmitz *et al.*, 2012) were kindly provided by Rainer E. Häusler (University of Cologne).
680 *gpt2-1* (AT1G61800; GK-454H06) and *srg3*/*gdpd1-1* (AT3G02040; SALK_087106) were
681 obtained from The Nottingham Arabidopsis Stock Centre (NASC) and were described
682 previously (Niewiadomski *et al.*, 2005; Cheng *et al.*, 2011). Primer sequences used for
683 genotyping are listed in Table S4. Homozygous insertion mutants were verified using the
684 following primer combinations: *PHR1* WT: PHR1_F/PHR1_R; *phr1-3* T-DNA:
685 LBb1/PHR1_R; *PHL1* WT: PHL1_F/PHL1_R; *phl1* T-DNA: PHL1_F/LB3; *TPT* WT:
686 TPT_F/TPT_R; *tpt-2* T-DNA: *tpt-2*_F/LBb1; *GPT2* WT: GPT2_F/GPT2_R; *gpt2-1* T-DNA:
687 GK-LB/GPT2_R; *SRG3* WT: qSRG3_F/SRG3_R; *srg3* T-DNA: qSRG3_F/LBb1. To generate
688 the *adg1 phr1 phl1* triple mutant, *adg1-1* was crossed to *phr1-3 phl1*. Homozygous *adg1-1*
689 mutants were identified by screening for starch-free phenotypes by iodine staining at the end of
690 the photoperiod. Homozygosity of the *phr1-1* allele was verified by Sanger sequencing
691 (Macrogen Europe, Amsterdam) of the PCR product of PHR1_F/PHR1_R using primer
692 PHR1_R.

693

694 **Cultivation conditions**

695 Seeds were stratified for 64 hours at 4°C in the dark. For vegetative growth, plants were
696 germinated and grown in an 8 h/16 h (light/dark) cycle and 23°C/22°C day/night temperature
697 on soil consisting of seeding compost, universal soil, and vermiculite mixed in a 3:3:1 ratio.
698 For high-light experiments, the plants were additionally fertilized once directly after pricking
699 at the age of 10 days using a complete mineral mixture (Wuxal Super, Aglukon Spezialduenger,

700 Duesseldorf, Germany) according to the manufacturer's instructions. For seedling experiments,
701 seeds were surface sterilized by chlorine gas exposure and transferred to solidified Arabidopsis
702 growth media as described in the figure legends. Seedlings were grown under 16 h/8 h light/dark
703 cycles. If not indicated otherwise, growth light was set to 90±10 µmol m^{-2} sec^{-1} (for seedling
704 growth and for experiments shown in Figure 1B-E), or 70±5 µmol m^{-2} s^{-1} (before high-light
705 treatments at 450±30 µmol m^{-2} s^{-1} of rosette plants), and monitored using an illuminance meter.
706 Growth and treatments of rosette plants for high-light experiments were conducted in a Percival
707 SE-41L plant growth incubator equipped with dimmable fluorescent lamps under temperature
708 control.

709

710 **P_i-limitation experiments**

711 For P_i-limitation experiments, seeds were germinated on medium containing MS salts
712 at full strength together with 0.8 % (w/v) phytoagar (Duchefa Biochemie, Haarlem, The
713 Netherlands) and 0.5 % (w/v) sucrose. After 5-10 days of growth (see figure legends), seedlings
714 were transferred to P_i media (0.5 % (w/v) sucrose; 20 mM 2-(N-Morpholino)-ethane sulphonic
715 acid; 2.5 mM KNO_3; 1 mM $MgSO_4$; 1 mM $Ca(NO_3)_2$; 2.5 mM KH_2PO_4; 25 µM Fe-EDTA;
716 35 µM H_3BO_3; 7 µM $MnCl_2$; 0.25 µM $CuSO_4$; 0.5 µM $ZNSO_4$; 0.1 µM $NaMoO_4$; 5 µM NaCl;
717 0.005 µM $CoCl_2$; pH 6) solidified by 0.8 % (w/v) agar (adopted from Härtel et al. (2000)). For
718 P_i depleting conditions, KH_2PO_4 was omitted, and Fe-EDTA was reduced to 10 µM in order to
719 minimize low-P_i induced iron toxicity (Ward *et al.*, 2008). Seedling shoots were harvested after
720 7-8 days of growth on P_i differing media (see figure legends). For the experiment shown in
721 Figures 1F and Supporting Information Fig. S3, P_i medium was used containing either 0.25 mM
722 KH_2PO_4/10 µM Fe-EDTA, 2.5 mM KH_2PO_4/25 µM Fe-EDTA, or 2.5 mM KH_2PO_4/25 µM Fe-
723 EDTA +50 mM sucrose. For the experiment shown in Figure 4F, seedlings were germinated on
724 MS salts at ½ strength without added sucrose and grown for 7 days before transfer to P_i-
725 differing conditions.

726

727 **Vector construction**

728 Standard molecular cloning procedures were applied. Primer sequences used for cloning
729 are listed in table S4. The firefly *LUCIFERASE* reporter plasmid *pBT10-proMGD3::LUC*$_{Firefly}$
730 and the *pHBTL-p35S::3HA-GFP* effector plasmid (Klecker *et al.*, 2014), as well as the *pBT10-*
731 *p35S::LUC*$_{Renilla}$ normalization plasmid (Bäumler *et al.*, 2019) have been described elsewhere.

732 For details on cloning *proSPX1*^{GC}, *proSRG3*, *proMGD3*, *proGPT2,* and the *PHR1* effector
733 construct, refer to the supplemental methods.

734

735 **Anthocyanin determination**

736 Anthocyanin contents were determined with few changes as described in
737 (Vandenbussche *et al.*, 2007). In brief, 40-70 mg of seedling shoots or rosette leaf material were
738 frozen in liquid nitrogen and ground in a bead mill (MM400, Retsch, Haan, Germany). The
739 frozen powder was resuspended in 300 µl of methanol containing 1 % HCl. After vortex-mixing
740 for 15 sec, cell debris was pelleted by centrifugation for 15 min at >14,000 g, 4°C. The
741 supernatant was mixed with 200 µl water and 500 µl chloroform by vortexing for 15 sec. After
742 15 min centrifugation at 17,900 g, 4°C, the upper phase was diluted in methanol to measure the
743 absorbance at 535 nm and 630 nm using a spectrophotometer (Specord 200 Plus, Analytik Jena,
744 Jena, Germany).

745

746 **Measurements of starch, soluble sugars, and adenylates**

747 Carbohydrates were determined by the Warburg optical test and adenylates were
748 assessed based on luciferase activity. Both procedures were described previously (Mustroph *et*
749 *al.*, 2006), for details see supplemental methods.

750

751 **Determination of P_i contents**

752 Free P_i was determined in leaf tissue based on the method described by (Ames, 1966)
753 with some modifications partially based on (Sakuraba *et al.*, 2018). For the experiment shown
754 in Figure 3D, leaf material was lyophilized prior to extraction, and 50 µl extraction buffer per
755 mg plant material was used. For details see supplemental methods.

756

757 **Non-aqueous fractionation of leaf material**

758 For the analysis of subcellular P_i distribution, 12 plant rosettes (total of >1 g) were
759 harvested into vials precooled by liquid nitrogen and dry ice, with an averaged harvesting time
760 of 3 seconds (max. 7 seconds) per rosette. The plant material was ground to a fine powder and
761 lyophilized. The freeze-dried powder was suspended in a mixture of tetrachlorethylene and n-
762 heptane and fractionated across a non-aqueous density gradient as described before (Hernandez

763 *et al.*, 2023). Following fractionation, marker enzyme activities for plastids (alkaline
764 pyrophosphatase), cytosol (UDP-glucose pyrophosphorylase), and vacuole (acidic
765 phosphatase) were determined photometrically. Phosphate amounts were determined as
766 described above for each fraction and correlated with the marker enzyme activities using the
767 using the NAFalyzer app (https://github.com/cellbiomaths/NAFalyzer).

768

769 **RNA extraction and cDNA synthesis**

770 Plant material was harvested under the respective experimental conditions and instantly
771 frozen in liquid nitrogen. The tissue was ground in a bead mill, and RNA was extracted using
772 Bioline TRIsure (Meridian Bioscience, Cincinnati, United States) according to the
773 manufacturer's instructions. The quality of the RNA was assessed by screening A_{260} and A_{280}.
774 For qRT-PCR analysis, 1 µg of RNA was treated with DNAse I (Thermo Fisher Scientific,
775 Waltham, United States) according to product instructions before application in reverse
776 transcription using oligo$(dT)_{15}$ and RevertAid Reverse Transcriptase (Thermo Fisher
777 Scientific). Complementary DNA was diluted by a factor of 50 for use as template in qPCR
778 analysis. qPCR was performed in technical triplicates using SsoAdvanced Universal SYBR
779 Green Supermix (Bio-Rad, Hercules, United States) on a CFX Connect Real-time System (Bio-
780 Rad). Transcript levels were normalized to the levels of *PP2A* transcript and calculated as
781 $1000 \cdot 2^{-\Delta CT}$. Primer sequences are listed in table S4.

782

783 **Protoplast isolation, transfection and transactivation assay**

784 Leaf mesophyll protoplasts were isolated using the "Tape-Arabidopsis Sandwich"
785 method (Wu *et al.*, 2009) with minor modifications. For details, see supplemental methods.

786

787 **Chlorophyll fluorescence measurements**

788 For the determination of the quantum yield of photosystem II photochemistry
789 $(F_m'-F')/F_m'$ (ΦPSII), as well as the maximum efficiency of photosystem II (F_v'/F_m'), and the
790 NPQ parameter (or SV_N; calculated by the Junior-PAM software using the Stern-Volmer
791 equation for fluorescence quenching, Gilmore and Yamamoto (1991)), pulse-amplitude-
792 modulated fluorescence measurements (PAM) of chlorophyll fluorescence were conducted
793 using a Junior-PAM (Walz, Effeltrich, Germany). Here, to calculate chlorophyll fluorescence
794 parameters using the saturating pulse method (Schreiber *et al.*, 1986), one large rosette leaf was

held between two magnets and subjected to 10 seconds of actinic light irradiance set to control light intensity (70±5 µmol m^{-2} sec^{-1}), followed by a saturation light pulse.

Lipid analysis

Lipid analysis was performed according to (Mueller *et al.*, 2015). Progenesis QI (version 2.1, Waters) was used for data pre-processing and PCA was performed in the MetaboAnalyst platform (version 6.0, www.metaboanalyst.ca).

Statistical analysis

Statistical analyses were performed with Microsoft Office Excel using the Real Statistics Resource Pack software (www.real-statistics.com). Two-factor ANOVA and hypergeometric testing were performed using RStudio (version 2024.09.1+394) available at https://www.r-project.org/.

Funding information

This research was funded by the University of Bayreuth and by the University of Würzburg.

Acknowledgements

We thank Stephan Clemens and Angelika Mustroph for helpful discussions and comments on the manuscript, as well as for providing infrastructure and equipment. We thank Susanne Berger for help with choosing experimental conditions used for lipid analyses.

Author contributions

M.K., conceptualization; A.F., T.N., and M.K., methodology; L.A., A.F., T.N., and M.K., formal analysis; L.A., A.F., T.N., A.H., M.M., and M.K., investigation; M.K., writing–original draft; all authors, writing–review and editing; A.F. and M.K., visualization; M.J.M and M.K., supervision; M.K., project administration.

823 # Competing interests

824 None declared.

825

826 # Data availability

827 The source data of lipid analyses are available in the Supporting information of this article.

828

829 # Supplemental Data

830 **Supporting Information Fig. S1** Phenotypes of *adg1-1 phr1-3 phl1* (TM).

831 **Supporting Information Fig. S2** Expression of selected P_i-starvation responsive genes
832 depends on *PHR1/PHL1* under P_i depletion.

833 **Supporting Information Fig. S3** Root growth of *adg1 phr1 phl1* and *adg1 tpt-2* responds to
834 exogenously applied sucrose.

835 **Supporting Information Fig. S4** *PHR1* transcript levels are not affected by short-time high-
836 light exposure.

837 **Supporting Information Fig. S5** Changes in sugar and starch contents under P_i depletion.

838 **Supporting Information Fig. S6** Monosaccharide levels after 20 min of high light.

839 **Supporting Information Fig. S7** Anthocyanin biosynthetic and regulatory gene expression
840 upon high light in WT and *phr1-1 phl1*.

841 **Supporting Information Fig. S8** Total levels of lipid classes in WT (Col-0) and *srg3* mutants
842 upon shift to high light (HL).

843 **Supporting Information Fig. S9** Contents of glycosylglycerol lipid species in WT (Col-0) and
844 *srg3* mutants upon shift to high light (HL) relative to fresh weight (FW).

845 **Supporting Information Fig. S10** Contents of glycerophospholipid species in WT (Col-0) and
846 *srg3* mutants upon shift to high light (HL) relative to fresh weight (FW).

847 **Supporting Information Fig. S11** Levels of zeaxanthin and putative glycosylated SQDG
848 determined in opposite ESI ion mode compared to Figure 5C.

849 **Supporting Information Fig. S12** Levels of triacylglycerol (TAG) species in WT (Col-0) and
850 *srg3* mutants upon shift to high light (HL).

851 **Supporting Information Fig. S13** Levels of high-temperature responsive transcripts *HSP70*
852 and *HSP18.2* in WT (Col-0) and *phr1-1 phl1* mutant plants upon high light treatment.

853 **Supporting Information Table S1** Annotated lipid features in WT (Col-0) and *srg3* mutants
854 following a shift to high light.

855 **Supporting Information Table S2** Lipid features whose levels were significantly altered upon
856 shifting to the WT (Col-0).

857 **Supporting Information Table S3** Heat-responsive lipid features whose levels differed
858 significantly between WT (Col-0) and *srg3* mutants.

859 **Supporting Information Table S4** List of primer sequences used in this study.

860 **Supplemental Methods and References**

861 # REFERENCES

862 **Abdelrahman M, Nishiyama R, Tran CD, Kusano M, Nakabayashi R, Okazaki Y,**
863 **Matsuda F, Chávez Montes RA, Mostofa MG, Li W, *et al.* 2021**. Defective cytokinin
864 signaling reprograms lipid and flavonoid gene-to-metabolite networks to mitigate high salinity
865 in Arabidopsis. *Proceedings of the National Academy of Sciences of the United States of*
866 *America* **118**.

867 **Ames BN**. **1966**. [10] Assay of inorganic phosphate, total phosphate and phosphatases. In:
868 Methods in Enzymology. 115–118.

869 **Athanasiou K, Dyson BC, Webster RE, Johnson GN**. **2010**. Dynamic acclimation of
870 photosynthesis increases plant fitness in changing environments. *Plant physiology* **152**: 366–
871 73.

872 **Baena-González E, Rolland F, Thevelein JM, Sheen J**. **2007**. A central integrator of
873 transcription networks in plant stress and energy signalling. *Nature* **448**: 938–42.

874 **Barragán-Rosillo AC, Peralta-Alvarez CA, Ojeda-Rivera JO, Arzate-Mejía RG, Recillas-**
875 **Targa F, Herrera-Estrella L**. **2021**. Genome accessibility dynamics in response to phosphate
876 limitation is controlled by the PHR1 family of transcription factors in Arabidopsis. *Proceedings*
877 *of the National Academy of Sciences of the United States of America* **118**.

878 **Bates PD**. **2016**. Understanding the control of acyl flux through the lipid metabolic network of
879 plant oil biosynthesis. *Biochimica et Biophysica Acta (BBA) - Molecular and Cell Biology of*
880 *Lipids* **1861**: 1214–1225.

881 **Bäumler J, Riber W, Klecker M, Müller L, Dissmeyer N, Weig AR, Mustroph A**. **2019**.
882 AtERF#111/ABR1 is a transcriptional activator involved in the wounding response. *The Plant*
883 *journal : for cell and molecular biology* **100**: 969–990.

884 **Bechtold U, Richard O, Zamboni A, Gapper C, Geisler M, Pogson B, Karpinski S,**
885 **Mullineaux PM**. **2008**. Impact of chloroplastic- and extracellular-sourced ROS on high light-
886 responsive gene expression in Arabidopsis. *Journal of experimental botany* **59**: 121–33.

887 **Borghi GL, Moraes TA, Günther M, Feil R, Mengin V, Lunn JE, Stitt M, Arrivault S**.
888 **2019**. Relationship between irradiance and levels of Calvin-Benson cycle and other
889 intermediates in the model eudicot Arabidopsis and the model monocot rice. *Journal of*
890 *Experimental Botany* **70**: 5809–5825.

891 **Burgos A, Szymanski J, Seiwert B, Degenkolbe T, Hannah MA, Giavalisco P, Willmitzer**

892 **L. 2011**. Analysis of short-term changes in the Arabidopsis thaliana glycerolipidome in
893 response to temperature and light. *Plant Journal* **66**: 656–668.

894 **Buseman CM, Tamura P, Sparks AA, Baughman EJ, Maatta S, Zhao J, Roth MR, Esch**
895 **SW, Shah J, Williams TD, *et al.* 2006**. Wounding stimulates the accumulation of glycerolipids
896 containing oxophytodienoic acid and dinor-oxophytodienoic acid in arabidopsis leaves. *Plant*
897 *Physiology* **142**: 28–39.

898 **Bustos R, Castrillo G, Linhares F, Puga MI, Rubio V, Pérez-Pérez J, Solano R, Leyva A,**
899 **Paz-Ares J. 2010**. A central regulatory system largely controls transcriptional activation and
900 repression responses to phosphate starvation in Arabidopsis. *PLoS genetics* **6**: e1001102.

901 **Castrillo G, Teixeira PJPL, Paredes SH, Law TF, de Lorenzo L, Feltcher ME, Finkel OM,**
902 **Breakfield NW, Mieczkowski P, Jones CD, *et al.* 2017**. Root microbiota drive direct
903 integration of phosphate stress and immunity. *Nature* **543**: 513–518.

904 **Cheng Y, Zhou W, El Sheery NI, Peters C, Li M, Wang X, Huang J. 2011**. Characterization
905 of the Arabidopsis glycerophosphodiester phosphodiesterase (GDPD) family reveals a role of
906 the plastid-localized AtGDPD1 in maintaining cellular phosphate homeostasis under phosphate
907 starvation. *Plant Journal* **66**: 781–795.

908 **Dang DTT, Nguyen LT, Tran A-T, Tran TTT, Tran T-A, Vo KTX, Jeon J-S, Van Vu T,**
909 **Kim J-Y, Nguyen NP, *et al.* 2025**. A novel glycerophosphodiester phosphodiesterase 13 is
910 involved in the phosphate starvation-induced phospholipid degradation in rice. *Plant*
911 *physiology and biochemistry : PPB* **228**: 110230.

912 **Demmig-Adams B, Adams WW. 1996**. The role of xanthophyll cycle carotenoids in the
913 protection of photosynthesis. *Trends in Plant Science* **1**: 21–26.

914 **Dietz K-J. 2015**. Efficient high light acclimation involves rapid processes at multiple
915 mechanistic levels. *Journal of experimental botany* **66**: 2401–14.

916 **Dietz KJ, Foyer C. 1986**. The relationship between phosphate status and photosynthesis in
917 leaves : Reversibility of the effects of phosphate deficiency on photosynthesis. *Planta* **167**:
918 376–81.

919 **Dietz K, Heber U. 1984**. Rate-limiting factors in leaf photosynthesis. I. Carbon fluxes in the
920 calvin cycle. *Biochimica et Biophysica Acta (BBA) - Bioenergetics* **767**: 432–443.

921 **Dietz K-J, Heber U. 1986**. Light and CO2 limitation of photosynthesis and states of the
922 reactions regenerating ribulose 1,5-bisphosphate or reducing 3-phosphoglycerate. *Biochimica*

923 *et Biophysica Acta (BBA) - Bioenergetics* **848**: 392–401.

924 **Dietz K-J, Turkan I, Krieger-Liszkay A**. **2016**. Redox- and Reactive Oxygen Species-
925 Dependent Signaling into and out of the Photosynthesizing Chloroplast. *Plant physiology* **171**:
926 1541–50.

927 **Dong J, Ma G, Sui L, Wei M, Satheesh V, Zhang R, Ge S, Li J, Zhang T-E, Wittwer C, *et***
928 ***al.* 2019**. Inositol Pyrophosphate InsP8 Acts as an Intracellular Phosphate Signal in
929 Arabidopsis. *Molecular plant* **12**: 1463–1473.

930 **Figueroa CM, Asencion Diez MD, Ballicora MA, Iglesias AA**. **2022**. Structure, function, and
931 evolution of plant ADP-glucose pyrophosphorylase. *Plant molecular biology* **108**: 307–323.

932 **Franco-Zorrilla JM, Martín AC, Leyva A, Paz-Ares J**. **2005**. Interaction between
933 phosphate-starvation, sugar, and cytokinin signaling in Arabidopsis and the roles of cytokinin
934 receptors CRE1/AHK4 and AHK3. *Plant Physiology* **138**: 847–857.

935 **Frank A, Matiolli CC, Viana AJC, Hearn TJ, Kusakina J, Belbin FE, Wells Newman D,**
936 **Yochikawa A, Cano-Ramirez DL, Chembath A, *et al.* 2018**. Circadian Entrainment in
937 Arabidopsis by the Sugar-Responsive Transcription Factor bZIP63. *Current biology : CB* **28**:
938 2597-2606.e6.

939 **Fredeen AL, Raab TK, Rao IM, Terry N**. **1990**. Effects of phosphorus nutrition on
940 photosynthesis in Glycine max (L.) Merr. *Planta* **181**: 399–405.

941 **Furbank RT, Lilley RM**. **1980**. Effects of inorganic phosphate on the photosynthetic carbon
942 reduction cycle in extracts from the stroma of pea chloroplasts. *Biochimica et biophysica acta*
943 **592**: 65–75.

944 **Giersch C, Robinson SP**. **1987**. Regulation of photosynthetic carbon metabolism during
945 phosphate limitation of photosynthesis in isolated spinach chloroplasts. *Photosynthesis*
946 *Research* **14**: 211–227.

947 **Gilmore AM, Yamamoto HY**. **1991**. Zeaxanthin Formation and Energy-Dependent
948 Fluorescence Quenching in Pea Chloroplasts under Artificially Mediated Linear and Cyclic
949 Electron Transport. *Plant physiology* **96**: 635–43.

950 **Goss R, Latowski D**. **2020**. Lipid Dependence of Xanthophyll Cycling in Higher Plants and
951 Algae. *Frontiers in plant science* **11**: 455.

952 **Han X, Yang Y, Wu Y, Liu X, Lei X, Guo Y**. **2017**. A bioassay-guided fractionation system
953 to identify endogenous small molecules that activate plasma membrane H + -ATPase activity

954 in Arabidopsis. *Journal of Experimental Botany* **68**: 2951–2962.

955 **Hanchi M, Thibaud M-C, Légeret B, Kuwata K, Pochon N, Beisson F, Cao A, Cuyas L,**
956 **David P, Doerner P, *et al.* 2018**. The Phosphate Fast-Responsive Genes PECP1 and PPsPase1
957 Affect Phosphocholine and Phosphoethanolamine Content. *Plant physiology* **176**: 2943–2962.

958 **Härtel H, Dormann P, Benning C. 2000**. DGD1-independent biosynthesis of extraplastidic
959 galactolipids after phosphate deprivation in Arabidopsis. *Proceedings of the National Academy*
960 *of Sciences of the United States of America* **97**: 10649–54.

961 **Häusler RE, Heinrichs L, Schmitz J, Flügge UI. 2014**. How sugars might coordinate
962 chloroplast and nuclear gene expression during acclimation to high light intensities. *Molecular*
963 *Plant* **7**: 1121–1137.

964 **Havaux M, Niyogi KK. 1999**. The violaxanthin cycle protects plants from photooxidative
965 damage by more than one mechanism. *Proceedings of the National Academy of Sciences of the*
966 *United States of America* **96**: 8762–8767.

967 **He Y, Zhang X, Li L, Sun Z, Li J, Chen X, Hong G. 2021**. SPX4 interacts with both PHR1
968 and PAP1 to regulate critical steps in phosphorus-status-dependent anthocyanin biosynthesis.
969 *The New phytologist* **230**: 205–217.

970 **Heinrichs L, Schmitz J, Flügge UI, Häusler RE. 2012**. The mysterious rescue of adg1-1/tpt-
971 2 - An Arabidopsis thaliana double mutant impaired in acclimation to high light - By
972 exogenously supplied sugars. *Frontiers in Plant Science* **3**.

973 **Heldt HW, Rapley L. 1970**. Specific transport of inorganic phosphate, 3-phosphoglycerate
974 and dihydroxyacetonephosphate, and of dicarboxylates across the inner membrane of spinach
975 chloroplasts. *FEBS letters* **10**: 143–148.

976 **Hendriks JHM, Kolbe A, Gibon Y, Stitt M, Geigenberger P. 2003**. ADP-glucose
977 pyrophosphorylase is activated by posttranslational redox-modification in response to light and
978 to sugars in leaves of Arabidopsis and other plant species. *Plant physiology* **133**: 838–49.

979 **Hernandez JS, Dziubek D, Schröder L, Seydel C, Kitashova A, Brodsky V, Nägele T. 2023**.
980 Natural variation of temperature acclimation of Arabidopsis thaliana. *Physiologia plantarum*
981 **175**: e14106.

982 **Hisamatsu Y, Goto N, Hasegawa K, Shigemori H. 2006**. Senescence-promoting effect of
983 arabidopside A. *Zeitschrift fur Naturforschung - Section C Journal of Biosciences* **61**: 363–366.

984 **Hu D, Cui R, Wang K, Yang Y, Wang R, Zhu H, He M, Fan Y, Wang L, Wang L, *et al.***

985 **2024**. The Myb73-GDPD2-GA2ox1 transcriptional regulatory module confers phosphate
986 deficiency tolerance in soybean. *Plant Cell* **36**: 2176–2200.

987 **Huang J, Zhao X, Chory J**. **2019**. The Arabidopsis Transcriptome Responds Specifically and
988 Dynamically to High Light Stress. *Cell Reports* **29**: 4186-4199.e3.

989 **Ibrahim A, Schütz AL, Galano JM, Herrfurth C, Feussner K, Durand T, Brodhun F,**
990 **Feussner I**. **2011**. The alphabet of galactolipids in Arabidopsis thaliana. *Frontiers in Plant*
991 *Science* **2**: 1–24.

992 **Karthikeyan AS, Varadarajan DK, Jain A, Held MA, Carpita NC, Raghothama KG**.
993 **2007**. Phosphate starvation responses are mediated by sugar signaling in Arabidopsis. *Planta*
994 **225**: 907–918.

995 **Klecker M, Gasch P, Peisker H, Dörmann P, Schlicke H, Grimm B, Mustroph A**. **2014**. A
996 Shoot-Specific Hypoxic Response of Arabidopsis Sheds Light on the Role of the Phosphate-
997 Responsive Transcription Factor PHOSPHATE STARVATION RESPONSE1. *Plant*
998 *physiology* **165**: 774–790.

999 **Kobayashi K, Awai K, Takamiya K, Ohta H**. **2004**. Arabidopsis type B
1000 monogalactosyldiacylglycerol synthase genes are expressed during pollen tube growth and
1001 induced by phosphate starvation. *Plant physiology* **134**: 640–8.

1002 **König J, Muthuramalingam M, Dietz K-J**. **2012**. Mechanisms and dynamics in the
1003 thiol/disulfide redox regulatory network: transmitters, sensors and targets. *Current opinion in*
1004 *plant biology* **15**: 261–8.

1005 **Krapp A, Berthomé R, Orsel M, Mercey-Boutet S, Yu A, Castaings L, Elftieh S, Major H,**
1006 **Renou JP, Daniel-Vedele F**. **2011**. Arabidopsis roots and shoots show distinct temporal
1007 adaptation patterns toward nitrogen starvation. *Plant Physiology* **157**: 1255–1282.

1008 **Kumar V, Sharma A, Bhardwaj R, Thukral AK**. **2019**. Elemental Composition of Plants
1009 and Multivariate Analysis. *National Academy Science Letters* **42**: 45–50.

1010 **Kunz HH, Häusler RE, Fettke J, Herbst K, Niewiadomski P, Gierth M, Bell K, Steup M,**
1011 **Flügge U-I, Schneider A**. **2010**. The role of plastidial glucose-6-phosphate/phosphate
1012 translocators in vegetative tissues of Arabidopsis thaliana mutants impaired in starch
1013 biosynthesis. *Plant biology (Stuttgart, Germany)* **12 Suppl 1**: 115–28.

1014 **Kunz H-H, Scharnewski M, Feussner K, Feussner I, Flügge U-I, Fulda M, Gierth M**. **2009**.
1015 The ABC transporter PXA1 and peroxisomal beta-oxidation are vital for metabolism in mature

1016 leaves of Arabidopsis during extended darkness. *The Plant cell* **21**: 2733–49.

1017 **Li H, He K, Zhang Z, Hu Y**. **2023**. Molecular mechanism of phosphorous signaling inducing
1018 anthocyanin accumulation in Arabidopsis. *Plant Physiology and Biochemistry* **196**: 121–129.

1019 **Li L, Sheen J**. **2016**. Dynamic and diverse sugar signaling. *Current Opinion in Plant Biology*
1020 **33**: 116–125.

1021 **Lin TP, Caspar T, Somerville C, Preiss J**. **1988**. Isolation and Characterization of a Starchless
1022 Mutant of Arabidopsis thaliana (L.) Heynh Lacking ADPglucose Pyrophosphorylase Activity.
1023 *Plant physiology* **86**: 1131–5.

1024 **Liu Z, Wu X, Wang E, Liu Y, Wang Y, Zheng Q, Han Y, Chen Z, Zhang Y**. **2022**. PHR1
1025 positively regulates phosphate starvation-induced anthocyanin accumulation through direct
1026 upregulation of genes F3'H and LDOX in Arabidopsis. *Planta* **256**: 42.

1027 **Liu Y, Xie Y, Wang H, Ma X, Yao W, Wang H**. **2017**. Light and Ethylene Coordinately
1028 Regulate the Phosphate Starvation Response through Transcriptional Regulation of
1029 PHOSPHATE STARVATION RESPONSE1. *The Plant cell* **29**: 2269–2284.

1030 **Liu S, Xu Z, Essemine J, Liu Y, Liu C, Zhang F, Iqbal Z, Qu M**. **2024**. GWAS unravels
1031 acid phosphatase ACP2 as a photosynthesis regulator under phosphate starvation conditions
1032 through modulating serine metabolism in rice. *Plant communications* **5**: 100885.

1033 **Mai NTP, Mai CD, Nguyen H Van, Le KQ, Duong LV, Tran TA, To HTM**. **2021**.
1034 Discovery of new genetic determinants of morphological plasticity in rice roots and shoots
1035 under phosphate starvation using GWAS. *Journal of plant physiology* **257**: 153340.

1036 **Marcus Y, Altman-Gueta H, Finkler A, Gurevitz M**. **2005**. Mutagenesis at two distinct
1037 phosphate-binding sites unravels their differential roles in regulation of Rubisco activation and
1038 catalysis. *Journal of Bacteriology* **187**: 4222–4228.

1039 **Matiolli CC, Soares RC, Alves HLS, Abreu IA**. **2022**. Turning the Knobs: The Impact of
1040 Post-translational Modifications on Carbon Metabolism. *Frontiers in plant science* **12**: 781508.

1041 **McClain AM, Sharkey TD**. **2019**. Triose phosphate utilization and beyond: From
1042 photosynthesis to end product synthesis. *Journal of Experimental Botany* **70**: 1755–1766.

1043 **Misson J, Raghothama KG, Jain A, Jouhet J, Block MA, Bligny R, Ortet P, Creff A,**
1044 **Somerville S, Rolland N, *et al.* 2005**. A genome-wide transcriptional analysis using
1045 Arabidopsis thaliana Affymetrix gene chips determined plant responses to phosphate
1046 deprivation. *Proceedings of the National Academy of Sciences of the United States of America*

1047 **102**: 11934–11939.

1048 **Moore M, Vogel MO, Dietz KJ**. **2014**. The acclimation response to high light is initiated
1049 within seconds as indicated by upregulation of AP2/ERF transcription factor network in
1050 Arabidopsis thaliana. *Plant Signaling and Behavior* **9**: 1–4.

1051 **Morcuende R, Bari R, Gibon Y, Zheng W, Pant BD, Bläsing O, Usadel B, Czechowski T,**
1052 **Udvardi MK, Stitt M, *et al.* 2007**. Genome-wide reprogramming of metabolism and regulatory
1053 networks of Arabidopsis in response to phosphorus. *Plant, Cell and Environment* **30**: 85–112.

1054 **Mueller SP, Krause DM, Mueller MJ, Fekete A**. **2015**. Accumulation of extra-chloroplastic
1055 triacylglycerols in Arabidopsis seedlings during heat acclimation. *Journal of Experimental*
1056 *Botany* **66**: 4517–4526.

1057 **Müller R, Morant M, Jarmer H, Nilsson L, Nielsen TH**. **2007**. Genome-wide analysis of the
1058 arabidopsis leaf transcriptome reveals interaction of phosphate and sugar metabolism. *Plant*
1059 *Physiology* **143**: 156–171.

1060 **Müller R, Nilsson L, Nielsen LK, Nielsen TH**. **2005**. Interaction between phosphate starvation
1061 signalling and hexokinase-independent sugar sensing in Arabidopsis leaves. *Physiologia*
1062 *Plantarum* **124**: 81–90.

1063 **Mustroph A, Boamfa EI, Laarhoven LJJ, Harren FJM, Albrecht G, Grimm B**. **2006**.
1064 Organ-specific analysis of the anaerobic primary metabolism in rice and wheat seedlings. I:
1065 Dark ethanol production is dominated by the shoots. *Planta* **225**: 103–14.

1066 **Niewiadomski P, Knappe S, Geimer S, Fischer K, Schulz B, Unte US, Rosso MG, Ache P,**
1067 **Flügge UI, Schneider A**. **2005**. The Arabidopsis plastidic glucose 6-phosphate/phosphate
1068 translocator GPT1 is essential for pollen maturation and embryo sac development. *Plant Cell*
1069 **17**: 760–775.

1070 **Nilsson AK, Fahlberg P, Johansson ON, Hamberg M, Andersson MX, Ellerström M**.
1071 **2016**. The activity of HYDROPEROXIDE LYASE 1 regulates accumulation of galactolipids
1072 containing 12-oxo-phytodienoic acid in Arabidopsis. *Journal of Experimental Botany* **67**:
1073 5133–5144.

1074 **Nilsson L, Lundmark M, Jensen PE, Nielsen TH**. **2012**. The Arabidopsis transcription factor
1075 PHR1 is essential for adaptation to high light and retaining functional photosynthesis during
1076 phosphate starvation. *Physiologia plantarum* **144**: 35–47.

1077 **Nilsson L, Müller R, Nielsen TH**. **2007**. Increased expression of the MYB-related transcription

1078 factor, PHR1, leads to enhanced phosphate uptake in Arabidopsis thaliana. *Plant, cell &*
1079 *environment* **30**: 1499–512.

1080 **Ohnishi M, Anegawa A, Sugiyama Y, Harada K, Oikawa A, Nakayama Y, Matsuda F,**
1081 **Nakamura Y, Sasaki R, Shichijo C, *et al.* 2018**. Molecular Components of Arabidopsis Intact
1082 Vacuoles Clarified with Metabolomic and Proteomic Analyses. *Plant & cell physiology* **59**:
1083 1353–1362.

1084 **Pant BD, Burgos A, Pant P, Cuadros-Inostroza A, Willmitzer L, Scheible WR**. **2015**. The
1085 transcription factor PHR1 regulates lipid remodeling and triacylglycerol accumulation in
1086 Arabidopsis thaliana during phosphorus starvation. *Journal of Experimental Botany* **66**: 1907–
1087 1918.

1088 **Preiss J**. **1984**. Starch, sucrose biosynthesis and partition of carbon in plants are regulated by
1089 orthophosphate and triose-phosphates. *Trends in Biochemical Sciences* **9**: 24–27.

1090 **Puga MI, Mateos I, Charukesi R, Wang Z, Franco-Zorrilla JM, de Lorenzo L, Irigoyen**
1091 **ML, Masiero S, Bustos R, Rodríguez J, *et al.* 2014**. SPX1 is a phosphate-dependent inhibitor
1092 of Phosphate Starvation Response 1 in Arabidopsis. *Proceedings of the National Academy of*
1093 *Sciences of the United States of America* **111**: 14947–52.

1094 **Raju AS, Kramer DM, Versaw WK**. **2024**. Genetically manipulated chloroplast stromal
1095 phosphate levels alter photosynthetic efficiency. *Plant Physiology* **196**: 385–396.

1096 **Ramaiah M, Jain A, Baldwin JC, Karthikeyan AS, Raghothama KG**. **2011**.
1097 Characterization of the phosphate starvation-induced glycerol-3-phosphate permease gene
1098 family in Arabidopsis. *Plant physiology* **157**: 279–91.

1099 **Ried MK, Wild R, Zhu J, Pipercevic J, Sturm K, Broger L, Harmel RK, Abriata LA,**
1100 **Hothorn LA, Fiedler D, *et al.* 2021**. Inositol pyrophosphates promote the interaction of SPX
1101 domains with the coiled-coil motif of PHR transcription factors to regulate plant phosphate
1102 homeostasis. *Nature communications* **12**: 384.

1103 **Riemer E, Qiu D, Laha D, Harmel RK, Gaugler P, Gaugler V, Frei M, Hajirezaei M-R,**
1104 **Laha NP, Krusenbaum L, *et al.* 2021**. ITPK1 is an InsP6/ADP phosphotransferase that
1105 controls phosphate signaling in Arabidopsis. *Molecular plant* **14**: 1864–1880.

1106 **Robinson S, Giersch C**. **1987**. Inorganic Phosphate Concentration in the Stroma of Isolated
1107 Chloroplasts and Its Influence on Photosynthesis. *Australian Journal of Plant Physiology* **14**:
1108 451.

1109 **van Rooijen R, Harbinson J, Aarts MGM**. **2018**. Photosynthetic response to increased
1110 irradiance correlates to variation in transcriptional response of lipid-remodeling and heat-shock
1111 genes. *Plant direct* **2**: e00069.

1112 **Rubio V, Linhares F, Solano R, Martín AC, Iglesias J, Leyva A, Paz-Ares J**. **2001**. A
1113 conserved MYB transcription factor involved in phosphate starvation signaling both in vascular
1114 plants and in unicellular algae. *Genes & development* **15**: 2122–33.

1115 **Sacharz J, Giovagnetti V, Ungerer P, Mastroianni G, Ruban A V. 2017**. The xanthophyll
1116 cycle affects reversible interactions between PsbS and light-harvesting complex II to control
1117 non-photochemical quenching. *Nature plants* **3**: 16225.

1118 **Safi A, Medici A, Szponarski W, Ruffel S, Lacombe B, Krouk G**. **2017**. The world according
1119 to GARP transcription factors. *Current Opinion in Plant Biology* **39**: 159–167.

1120 **Sakuraba Y, Kanno S, Mabuchi A, Monda K, Iba K, Yanagisawa S**. **2018**. A phytochrome-
1121 B-mediated regulatory mechanism of phosphorus acquisition. *Nature plants* **4**: 1089–1101.

1122 **Santarius KA, Heber U**. **1965**. Changes in the intracellular levels of ATP, ADP, AMP and P1
1123 and regulatory function of the adenylate system in leaf cells during photosynthesis. *Biochimica*
1124 *et biophysica acta* **102**: 39–54.

1125 **Schmitz J, Heinrichs L, Scossa F, Fernie AR, Oelze M-L, Dietz K-J, Rothbart M, Grimm**
1126 **B, Flügge U-I, Häusler RE**. **2014**. The essential role of sugar metabolism in the acclimation
1127 response of Arabidopsis thaliana to high light intensities. *Journal of experimental botany* **65**:
1128 1619–36.

1129 **Schmitz J, Schöttler MA, Krueger S, Geimer S, Schneider A, Kleine T, Leister D, Bell K,**
1130 **Flügge U-I, Häusler RE**. **2012**. Defects in leaf carbohydrate metabolism compromise
1131 acclimation to high light and lead to a high chlorophyll fluorescence phenotype in Arabidopsis
1132 thaliana. *BMC plant biology* **12**: 8.

1133 **Schneider A, Häusler RE, Kolukisaoglu U, Kunze R, van der Graaff E, Schwacke R,**
1134 **Catoni E, Desimone M, Flügge U-I**. **2002**. An Arabidopsis thaliana knock-out mutant of the
1135 chloroplast triose phosphate/phosphate translocator is severely compromised only when starch
1136 synthesis, but not starch mobilisation is abolished. *The Plant journal : for cell and molecular*
1137 *biology* **32**: 685–99.

1138 **Schreiber U, Schliwa U, Bilger W**. **1986**. Continuous recording of photochemical and non-
1139 photochemical chlorophyll fluorescence quenching with a new type of modulation fluorometer.
1140 *Photosynthesis Research* **10**: 51–62.

1141 **Sharkey TD**. **1985**. O(2)-insensitive photosynthesis in c(3) plants : its occurrence and a
1142 possible explanation. *Plant physiology* **78**: 71–5.

1143 **Sivak MN, Walker DA**. **1986**. Photosynthesis in vivo can be limited by phosphate supply. *New*
1144 *Phytologist* **102**: 499–512.

1145 **Stitt M, Huber S, Kerr P**. **1987**. Control of Photosynthetic Sucrose Formation. In:
1146 Photosynthesis. Elsevier, 327–409.

1147 **Stitt M, Wirtz W, Heldt HW**. **1983**. Regulation of Sucrose Synthesis by Cytoplasmic
1148 Fructosebisphosphatase and Sucrose Phosphate Synthase during Photosynthesis in Varying
1149 Light and Carbon Dioxide. *Plant physiology* **72**: 767–74.

1150 **Sun L, Song L, Zhang Y, Zheng Z, Liu D**. **2016**. Arabidopsis PHL2 and PHR1 Act
1151 Redundantly as the Key Components of the Central Regulatory System Controlling
1152 Transcriptional Responses to Phosphate Starvation. *Plant physiology* **170**: 499–514.

1153 **Suzuki N, Devireddy AR, Inupakutika MA, Baxter A, Miller G, Song L, Shulaev E, Azad**
1154 **RK, Shulaev V, Mittler R**. **2015**. Ultra-fast alterations in mRNA levels uncover multiple
1155 players in light stress acclimation in plants. *The Plant journal : for cell and molecular biology*
1156 **84**: 760–72.

1157 **Thibaud M-C, Arrighi J-F, Bayle V, Chiarenza S, Creff A, Bustos R, Paz-Ares J, Poirier**
1158 **Y, Nussaume L**. **2010**. Dissection of local and systemic transcriptional responses to phosphate
1159 starvation in Arabidopsis. *The Plant journal : for cell and molecular biology* **64**: 775–89.

1160 **Vandenbussche F, Habricot Y, Condiff AS, Maldiney R, Van Der Straeten D, Ahmad M**.
1161 **2007**. HY5 is a point of convergence between cryptochrome and cytokinin signalling pathways
1162 in Arabidopsis thaliana. *Plant Journal* **49**: 428–441.

1163 **Verma L, Pandey M, Bhatia C, Mehra P, Singh B, Giri J**. **2025**. Phosphate deficiency
1164 inducible OsGDPD5 affects root growth by regulating sugar-auxin crosstalk. *The Plant*
1165 *journal : for cell and molecular biology* **121**: e17249.

1166 **Vogel MO, Moore M, König K, Pecher P, Alsharafa K, Lee J, Dietz KJ**. **2014**. Fast
1167 retrograde signaling in response to high light involves metabolite export, MITOGEN-
1168 ACTIVATED PROTEIN KINASE6, and AP2/ERF transcription factors in Arabidopsis. *Plant*
1169 *Cell* **26**: 1151–1165.

1170 **Vu HS, Roth MR, Tamura P, Samarakoon T, Shiva S, Honey S, Lowe K, Schmelz EA,**
1171 **Williams TD, Welti R**. **2014**. Head-group acylation of monogalactosyldiacylglycerol is a

1172 common stress response, and the acyl-galactose acyl composition varies with the plant species
1173 and applied stress. *Physiologia Plantarum* **150**: 517–528.

1174 **Walker DA, Osmond CB**. **1986**. Measurement of photosynthesis in vivo with a leaf disc
1175 electrode: correlations between light dependence of steady-state photosynthetic O 2 evolution
1176 and chlorophyll a fluorescence transients. *Proceedings of the Royal Society of London. Series*
1177 *B. Biological Sciences* **227**: 267–280.

1178 **Walker DA, Sivak MN**. **1986**. Photosynthesis and phosphate: a cellular affair? *Trends in*
1179 *Biochemical Sciences* **11**: 176–179.

1180 **Wang Z, Zheng Z, Zhu Y, Kong S, Liu D**. **2023**. PHOSPHATE RESPONSE 1 family
1181 members act distinctly to regulate transcriptional responses to phosphate starvation. *Plant*
1182 *Physiology* **191**: 1324–1343.

1183 **Ward JT, Lahner B, Yakubova E, Salt DE, Raghothama KG**. **2008**. The effect of iron on
1184 the primary root elongation of Arabidopsis during phosphate deficiency. *Plant physiology* **147**:
1185 1181–91.

1186 **Weber H**. **2002**. Fatty acid-derived signals in plants. *Trends in plant science* **7**: 217–24.

1187 **Weise SE, Liu T, Childs KL, Preiser AL, Katulski HM, Perrin-Porzondek C, Sharkey TD**.
1188 **2019**. Transcriptional Regulation of the Glucose-6-Phosphate/Phosphate Translocator 2 Is
1189 Related to Carbon Exchange Across the Chloroplast Envelope. *Frontiers in plant science* **10**:
1190 827.

1191 **Wild R, Gerasimaite R, Jung JY, Truffault V, Pavlovic I, Schmidt A, Saiardi A, Jacob**
1192 **Jessen H, Poirier Y, Hothorn M, *et al.* 2016**. Control of eukaryotic phosphate homeostasis by
1193 inositol polyphosphate sensor domains. *Science* **352**: 986–990.

1194 **Wojciechowska I, Mukherjee T, Knox-Brown P, Hu X, Khosla A, Subedi B, Ahmad B,**
1195 **Mathews GL, Panagakis AA, Thompson KA, *et al.* 2024**. Arabidopsis PROTODERMAL
1196 FACTOR2 binds lysophosphatidylcholines and transcriptionally regulates phospholipid
1197 metabolism. *New Phytologist*.

1198 **Woodrow IE, Raymond Ellis J, Jellings A, Foyer CH**. **1984**. Compartmentation and fluxes
1199 of inorganic phosphate in photosynthetic cells. *Planta* **161**: 525–30.

1200 **Wu P, Ma L, Hou X, Wang M, Wu Y, Liu F, Deng XW**. **2003**. Phosphate starvation triggers
1201 distinct alterations of genome expression in arabidopsis roots and leaves. *Plant Physiology* **132**:
1202 1260–1271.

1203 **Wu FH, Shen SC, Lee LY, Lee SH, Chan MT, Lin CS**. **2009**. Tape-arabidopsis sandwich -
1204 A simpler arabidopsis protoplast isolation method. *Plant Methods* **5**: 1–10.

1205 **Xu L, Zhao H, Wan R, Liu Y, Xu Z, Tian W, Ruan W, Wang F, Deng M, Wang J, *et al.***
1206 **2019**. Identification of vacuolar phosphate efflux transporters in land plants. *Nature Plants* **5**:
1207 84–94.

1208 **Yang Y, Benning C**. **2018**. Functions of triacylglycerols during plant development and stress.
1209 *Current Opinion in Biotechnology* **49**: 191–198.

1210 **Yang B, Peng Y, Zhang G, Liu R, Hao S, Ren Y, Lu S, Wang X, Guo L**. **2025**. Regulation
1211 of glucosylceramide synthase and sphingolipid remodeling in the plant response to phosphate
1212 deficiency. *The Plant cell* **37**.

1213 **Zhou J, Jiao F, Wu Z, Li Y, Wang X, He X, Zhong W, Wu P**. **2008**. OsPHR2 is involved in
1214 phosphate-starvation signaling and excessive phosphate accumulation in shoots of plants. *Plant*
1215 *physiology* **146**: 1673–86.

1216 **Zhu J, Lau K, Puschmann R, Harmel RK, Zhang Y, Pries V, Gaugler P, Broger L, Dutta**
1217 **AK, Jessen HJ, *et al.* 2019**. Two bifunctional inositol pyrophosphate kinases/phosphatases
1218 control plant phosphate homeostasis. *eLife* **8**: 1–25.

1219 **Zirngibl M-E, Araguirang GE, Kitashova A, Jahnke K, Rolka T, Kühn C, Nägele T,**
1220 **Richter AS**. **2023**. Triose phosphate export from chloroplasts and cellular sugar content
1221 regulate anthocyanin biosynthesis during high light acclimation. *Plant communications* **4**:
1222 100423.

1223

Figures

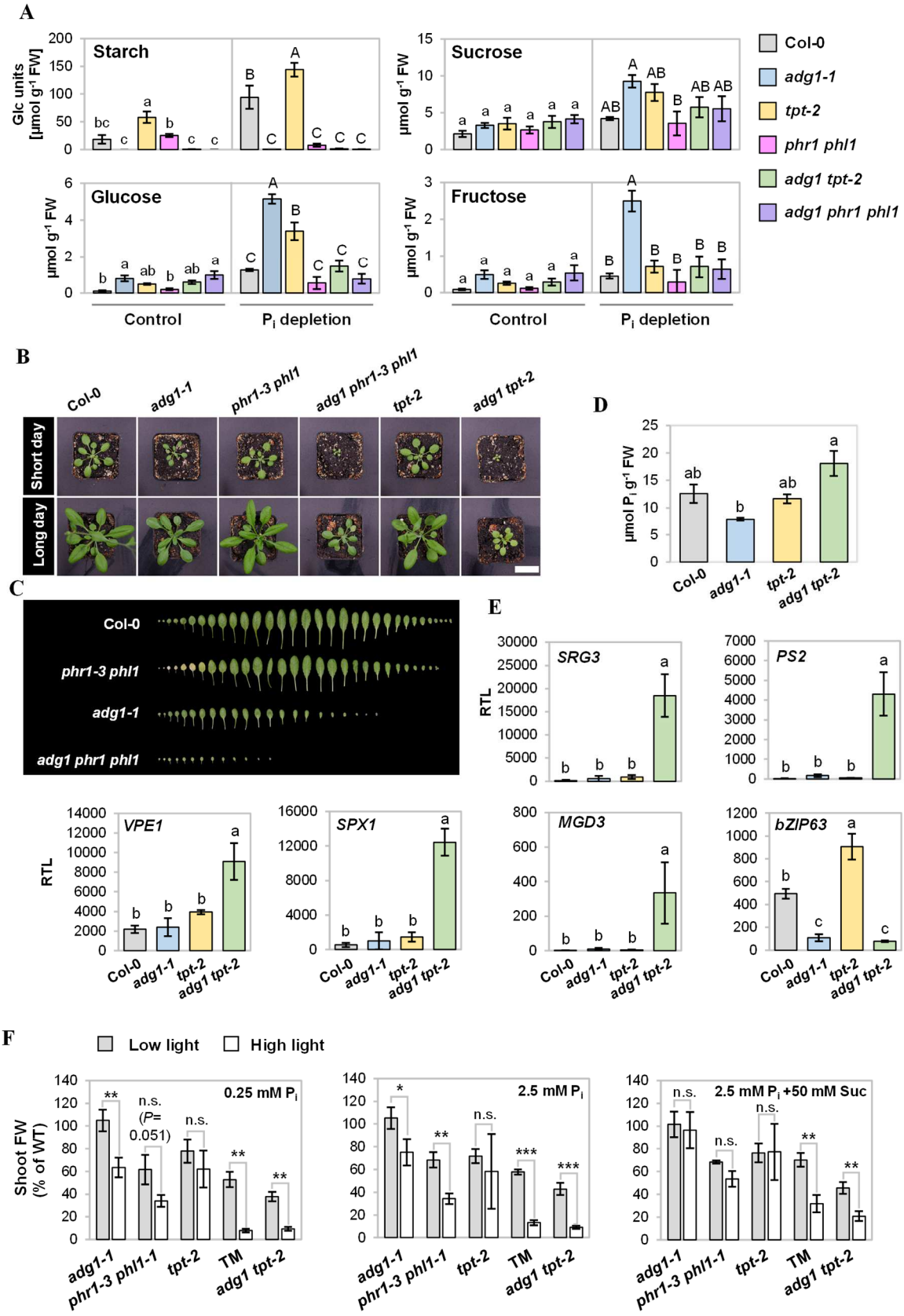
A
Starch
Glc units [µmol g-1 FW]
Sucrose
µmol g-1 FW
Glucose
Fructose
Control
Pi depletion
Col-0
adg1-1
tpt-2
phr1 phl1
adg1 tpt-2
adg1 phr1 phl1
B
Col-0
adg1-1
phr1-3 phl1
adg1 phr1-3 phl1
tpt-2
adg1 tpt-2
Short day
Long day
D
µmol Pi g-1 FW
C
Col-0
phr1-3 phl1
adg1-1
adg1 phr1 phl1
E
SRG3
PS2
VPE1
SPX1
MGD3
bZIP63
RTL
F
Low light
High light
Shoot FW (% of WT)
0.25 mM Pi
2.5 mM Pi
2.5 mM Pi +50 mM Suc
n.s.
(P= 0.051)
adg1-1
phr1-3 phl1-1
tpt-2
TM
adg1 tpt-2

1226 **Figure 1** Mutants with defects in photoassimilate partitioning show altered P_i responses. **A,**
1227 Contents of glucose, fructose, sucrose, and starch in shoots upon P_i depletion relative to fresh
1228 weight (**FW**). Seedlings of WT (Col-0), *adg1-1*, *tpt-2*, *phr1-3 phl1*, *adg1 tpt-2* and
1229 *adg1 phr1-3 phl1* genotype were grown for 10 days on rich medium containing 0.5 % sucrose
1230 before transfer to media with 0.5 % sucrose and either 2.5 mM (**Control**) or 0 mM (**P_i**
1231 **depletion**) KH_2PO_4 added. Growth was continued for 7 days. Pools of seedling shoots were
1232 harvested 10.25 h after onset of the 16-h photoperiod. Means ± standard deviations; n = 3
1233 independent experiments. Letter code indicates statistical differences at $P < 0.05$. One-way
1234 ANOVA with Tukey HSD follow-up test and Bonferroni alpha correction for contrasts. **B, C,**
1235 Phenotype of the *adg1 phr1 phl1* triple mutant. Plants were grown at 23°C and a light intensity
1236 of 100±10 µmol m^{-2} s^{-1}. **B,** Rosette habitus of plants grown under short-day (8 h light period)
1237 and long-day (16 h light period) conditions. Pictures were taken of representative plants after
1238 27 (short day) and 25 (long day) days of growth. Bar, 2.5 cm. **C,** Leaves of 42 day-old plants
1239 grown under an 8-h light regime were aligned according to age (starting with the cotyledons on
1240 the left hand side). Background was manually removed for better visualization. **D, E,**
1241 Constitutive P_i-starvation transcription in rosette leaves of *adg1 tpt-2*. Plants were grown on
1242 soil at a photon flux density of 90±10 µmol m^{-2} s^{-1} and sampled 135 min after onset of the 8-h
1243 photoperiod after 5 weeks of growth. **D,** P_i contents of rosette leaves. Means ± standard
1244 deviations are depicted. n = 3 independent experiments. Kruskal-Wallis test with DUNN‘s
1245 follow-up test and DUNN/Sidak alpha correction for contrasts; $P < 0.01$. **E,** qRT-PCR analysis
1246 of P_i starvation responsive genes in rosette leaves of WT, *adg1-1*, *tpt-2*, and *adg1 tpt-2*.
1247 Transcript levels are $1000 \cdot 2^{-\Delta CT}$ relative to *PP2A*. Bars show means ± standard deviations. n =
1248 3 independent experiments. One-way ANOVA with Tukey HSD follow-up test and Bonferroni
1249 alpha correction for contrasts; $P < 0.01$. **F**, High-light sensitivity of *adg1-1*, *phr1-3 phl1* and
1250 derived mutants. Seedlings were grown for two weeks in a 16/8 h (light/dark) cycle under low
1251 light (60±5 µmol m^{-2} s^{-1}) or high light (350±30 µmol m^{-2} s^{-1}) on agar-solidified media
1252 containing 0.25 mM P_i, 2.5 mM P_i, or 2.5 mM P_i +50 mM sucrose. Shoot FW were calculated
1253 as percent of mean shoot FW of WT seedlings grown under the respective conditions. Bars
1254 represent means ± standard deviations; n = 3 independent experiments comprising means of
1255 each 4-8 seedling shoots. Statistical analyses were performed using Student’s t test with 2-tailed
1256 distribution, unpaired with unequal variance. Significant differences between data are indicated
1257 as ***$P < 0.001$, **$P < 0.01$, *$P < 0.05$, n.s., not significant.

1258

A

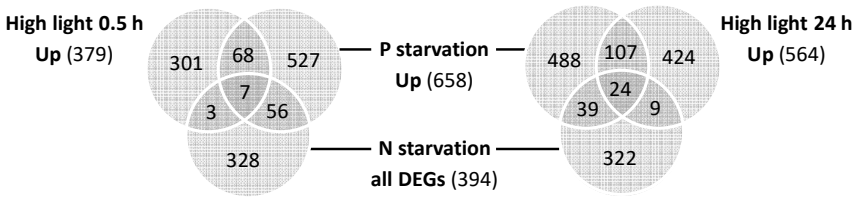
High light 0.5 h
Up (379)
301
68
527
7
3
56
328
P starvation
Up (658)
488
107
424
24
39
9
322
N starvation
all DEGs (394)
High light 24 h
Up (564)

B

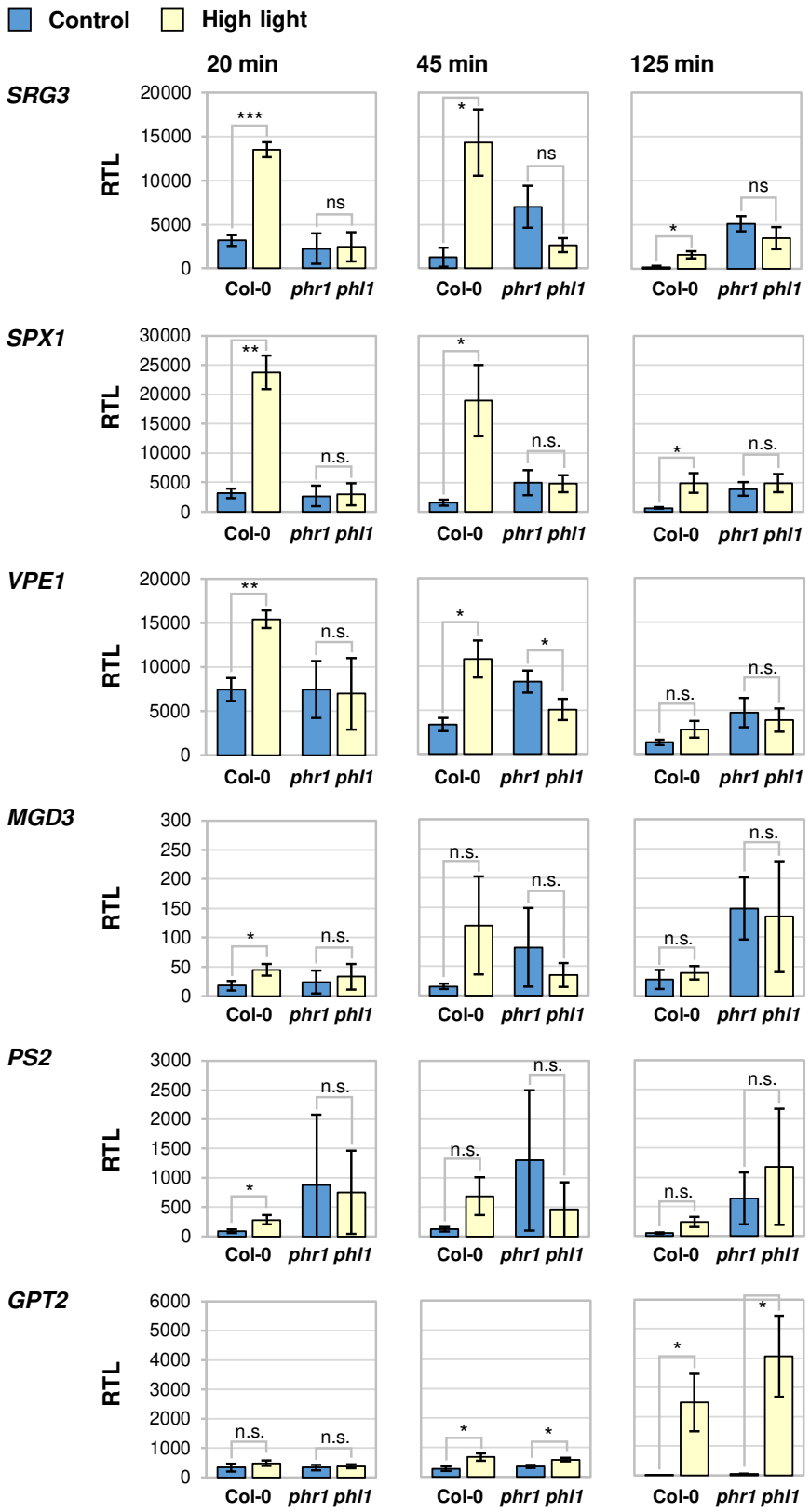
Control
High light
20 min
45 min
125 min
SRG3
SPX1
VPE1
MGD3
PS2
GPT2
RTL
Col-0
phr1 phl1
***
**
*
ns
n.s.

1260 **Figure 2** High light triggers P_i-depletion responsive gene expression. **A**, Overlap of differential
1261 gene expression in shoots upon high light, P_i starvation, and nitrogen starvation. Venn diagrams
1262 show numbers of transcripts upregulated by high light or P_i starvation, and of genes
1263 differentially expressed under N starvation. Transcript data are taken from Huang et al. (2019)
1264 (high light), Bustos et al. (2010) (P_i depletion), and Krapp et al. (2011) (N depletion). **B**, qRT-
1265 PCR analyses of selected transcripts in rosette leaves from WT (Col-0) and *phr1-1 phl1*
1266 mutants. Plants were grown on soil at 23°C for 5 weeks in an 8-h light regime at
1267 70±5 µmol m^{-2} s^{-1} before light intensity was set to 450±30 µmol m^{-2} s^{-1} (High light, yellow bars)
1268 starting 1 h after onset of the photoperiod on day 36. The control group was kept at 70±5 µmol
1269 m^{-2} s^{-1} (blue bars). Each 2-3 fully developed leaves (leaves no. 10-13) were harvested per sample
1270 at the indicated treatment times. Transcript levels were calculated relative to *PP2A* as
1271 $1000 \cdot 2^{-\Delta CT}$. Bars represent means ± standard deviations, n = 3 independent experiments.
1272 Statistical analyses were performed using Student's *t* test with 2-tailed distribution, unpaired
1273 with unequal variance. Significant differences are indicated as ***P <0.001, **P <0.01, *P
1274 <0.05, n.s., not significant.

1275

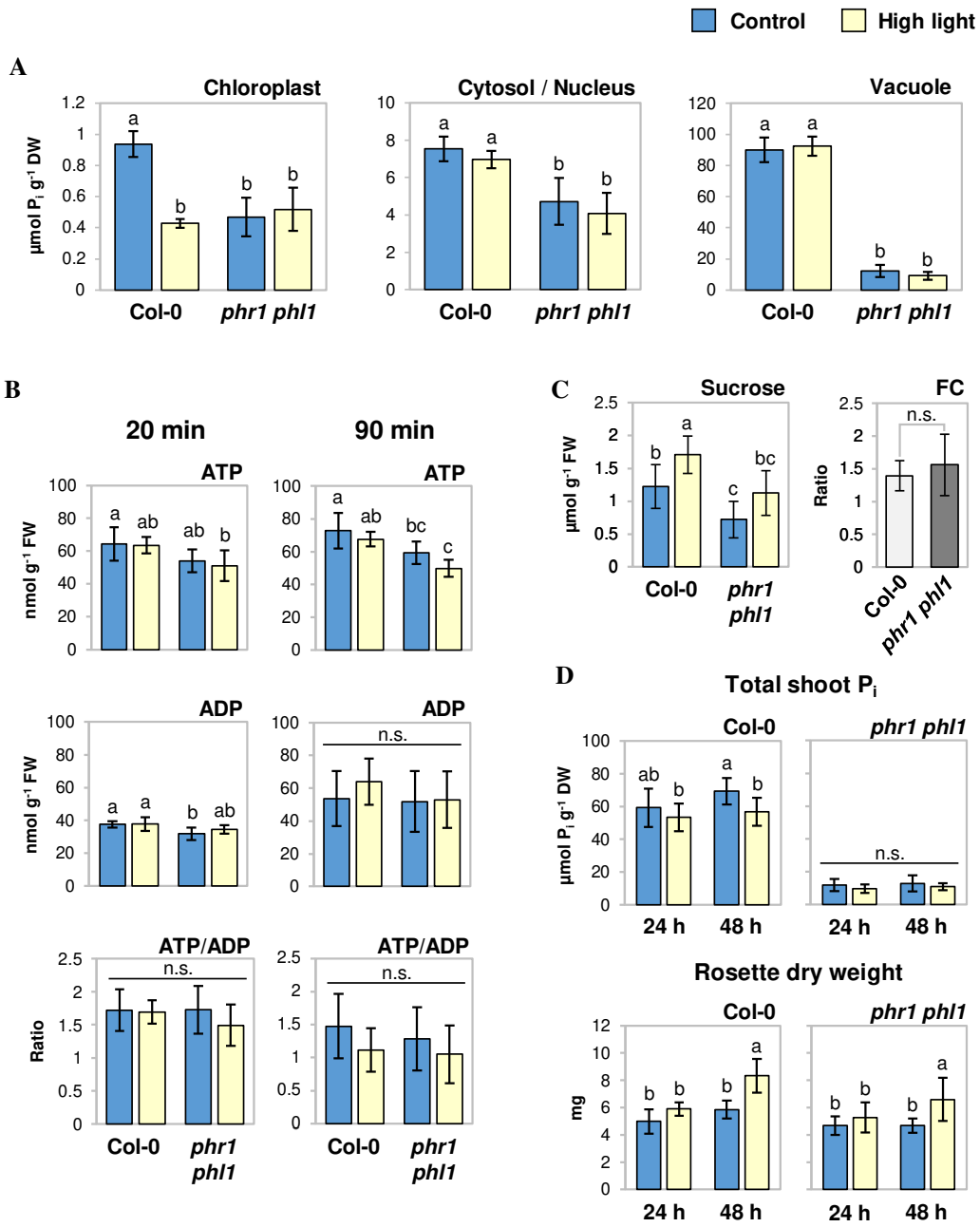

Figure 3 High light affects cellular P_i pools and sucrose levels. **A-C**, Plants were grown and treated as described in Fig. 2B. **A**, Subcellular P_i concentrations in WT and *phr1-1 phl1* mutant plants upon high light relative to dry weight (**DW**). Rosettes were harvested after 20 min of treatment. P_i contents were determined following non-aqueous fractionation of cellular compartments. n = 4 (*phr1-1 phl1*) or 5 (Col-0) independent experiments. **B,** Changes in ATP/ADP levels after shift to high light relative to fresh weight (**FW**). n = 6 plants from 3 (90 min) or 4 (20 min) independent experiments. **C**, Sucrose levels upon 20 min of high light; n = 8 plants from 4 independent experiments; absolute values and fold changes (**FC**, high light/control) are shown. Significant difference in FC was tested using Student's t test with 2-tailed distribution, unpaired with unequal variance. **D,** High light affects total shoot P_i and

1287 growth rates on the medium-term. WT and *phr1-1 phl1* mutants were grown for 4 weeks as
1288 described for Fig. 2B before light intensity was shifted to 450±30 µmol m^{-2} s^{-1} (high light) at
1289 4 h after onset of the photoperiod. Control plants were kept under growth light conditions (70±5
1290 µmol m^{-2} s^{-1}). Material was harvested after 24 and 48 h. Total P_i contents in rosettes relative to
1291 DW and average rosette DWs are depicted; n = 10 plants from 5 individual experiments. All
1292 bars show means ± standard deviations. Except for FC shown in **C**, all statistical analysis were
1293 performed using 2-factor ANOVA with Tukey HSD post-hoc test; $P < 0.05$; n.s., not significant.

1294

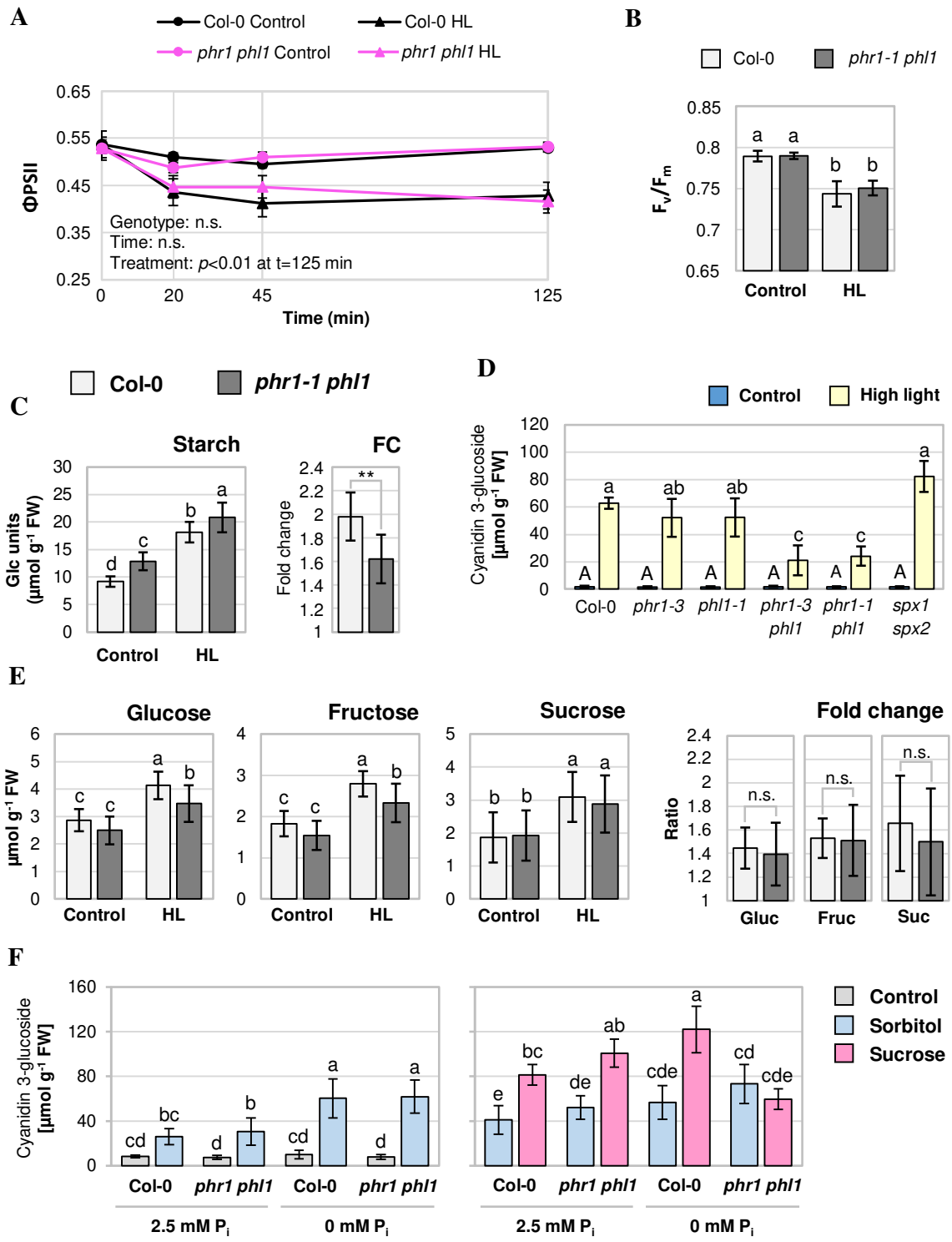

Figure 4 *phr1-1 phl1* mutants show altered carbohydrate responses. Unless specified, plants were grown and treated as described for Fig. 2B. Data points and bars depict means ± standard deviations. **A, B**, PAM measurements were performed to determine the effect of high light (**HL**) on chlorophyll a fluorescence parameters. n = 3 independent experiments (representing means of each 3 leaves measured). **A,** Quantum yield of photosystem II photochemistry (**ΦPSII**) in light-adapted leaves after 20, 45, and 125 min of treatment. Significance was tested using One-

1302 way ANOVA with Tukey HSD follow-up test and Bonferroni alpha correction for contrasts;
1303 n.s., not significant. **B,** Plants subjected to high-light stress were dark-adapted for 20 min after
1304 125 min of stress duration to determine the maximum efficiency of photosystem II (F_v/F_m). 2-
1305 factor ANOVA with Tukey HSD post-hoc test; $P < 0.05$. **C, E**, Changes in carbohydrate levels
1306 in WT (Col-0) and *phr1-1 phl1* mutants after 90 min of high-light treatment. 2-factor ANOVA
1307 with Tukey HSD post-hoc test; $P < 0.05$. Fold changes (**FC**) of sugar/starch contents were
1308 calculated for each genotype as HL/mean of control. Statistical analyses of FC were performed
1309 with Student‘s *t* test with two-tailed distribution, unpaired with unequal variance. Significant
1310 differences are indicated as ** $P < 0.01$, n.s. not significant. **C**, Starch levels relative to fresh
1311 weight (**FW**); $n = 9$ plants from 3 independent experiments. **D**, Anthocyanin (cyanidin 3-
1312 glucoside) levels after 3 days of high-light exposure. Plants were grown for 32 days until onset
1313 of the treatment. Leaf material was harvested after additional 70 h. Pigment contents were
1314 calculated relative to FW. $n = 3$ independent experiments; statistical analyses were conducted
1315 for each treatment group using One-way ANOVA with Tukey HSD follow-up test and
1316 Bonferroni alpha correction for contrasts, $P < 0.01$. **E**, Levels of glucose, fructose, and sucrose
1317 after 90 min of high-light treatment. $n = 11$-12 plants from 4 independent experiments. **F**,
1318 *phr1-1 phl1* mutants are defective in sugar-induced anthocyanin production under P_i-limiting
1319 conditions. Seedlings were grown on nutrient-rich media (no sucrose or sorbitol added) for 7
1320 days under a 16-h light regime before transfer to media with either 0 or 2.5 mM KH_2PO_4 added
1321 and containing either no additives (control), 90 mM sucrose, or 160.7 mM sorbitol (same
1322 osmotic strength). Seedling shoots were harvested for anthocyanin determination after 67 h of
1323 growth on differing media. $n = 6$ pools of seedling shoots from 3 independent experiments; 2-
1324 factor ANOVA with Tukey post-hoc test; $P < 0.05$.

1325

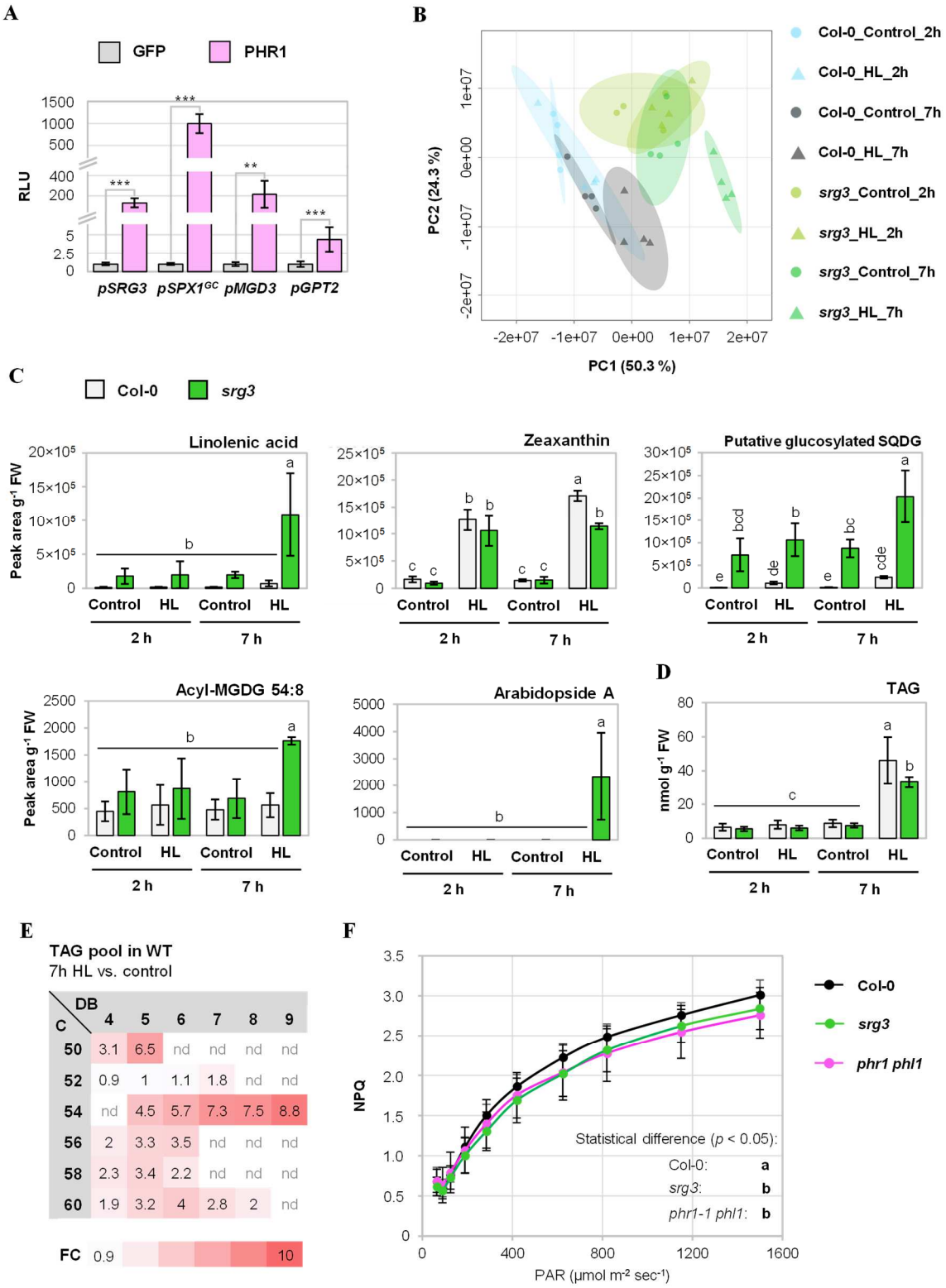

Figure 5 Effect of *srg3* mutation on the lipid composition upon light increase. **A,** Promoter transactivation assay in mesophyll protoplasts showing that the promoters of *SPX1*, *MGD3*, and *SRG3* are activated by PHR1. Promoter sequences were fused to the firefly *LUC* reporter gene (*proSRG3::LUC*$_{Firefly}$; *proSPX1*^{GC}*::LUC*$_{Firefly}$; *proMGD3::LUC*$_{Firefly}$, *proGPT2::LUC*$_{Firefly}$) and

1332 co-transfected with either *PHR1* or *GFP*. Luminescence units were normalized to the
1333 luminescence of *Renilla LUC* which was additionally co-expressed from the Cauliflower
1334 mosaic virus *35S* promoter, and calculated relative to the luminescence level of GFP-expressing
1335 samples. **RLU**, relative luminescence level. Results for each promoter construct are from
1336 independently triplicated experiments. Means ± standard deviations; n = 6 from 3 independent
1337 experiments. One-way ANOVA with Tukey HSD follow-up test and Bonferroni alpha
1338 correction for contrasts; ***P < 0.001, **P < 0.01. **B-E**, Plants of WT (Col-0) and *srg3*
1339 genotype were grown and treated as described for Fig. 2B, but leaves were harvested at 2 and
1340 7 h of treatment. Lipid species were analyzed using LC-MS. **B**, Principal component analysis
1341 of samples from 2 h and 7 h high-light (**HL**) treated or control plants of WT and *srg3* genotype.
1342 **C**, Levels of *srg3*-dependent HL-responsive lipid features normalized to leaf fresh weight
1343 (**FW**). n = 4 independent experiments, except for acyl-MGDG: n = 3-4. **D, E,** n = 3-4. **D,**
1344 Contents of triacylglycerols (**TAG**) in WT and *srg3* leaves after high-light treatments. **E**,
1345 Changes in TAG pools upon 7 h of light increase (7 h HL vs. 7 h control) in the WT. Fold
1346 changes (Col-0_HL_7h/Col-0_C_7h) are indicated by color code and were calculated for TAG
1347 species sorted by the total number of carbon atoms of the acyl chains (**C**) and the total number
1348 of double bonds (**DB**). **nd**, not detected. **F**, Light response of the NPQ parameter measured by
1349 PAM chlorophyll fluorometry. Plants of WT (Col-0), *srg3*, and *phr1-1 phl1* genotype were
1350 grown for 40 days in an 8-h light regime at 70±5 µmol m^{-2} s^{-1} and dark-adapted for ≥30 min
1351 before measurement. NPQ was plotted against the fluence rate of photosynthetically active
1352 radiation (**PAR**). n = 3 independent experiments representing means of 2 plants. **C-F**, 2-factor
1353 ANOVA with Tukey HSD post-hoc test; P < 0.05.

1354

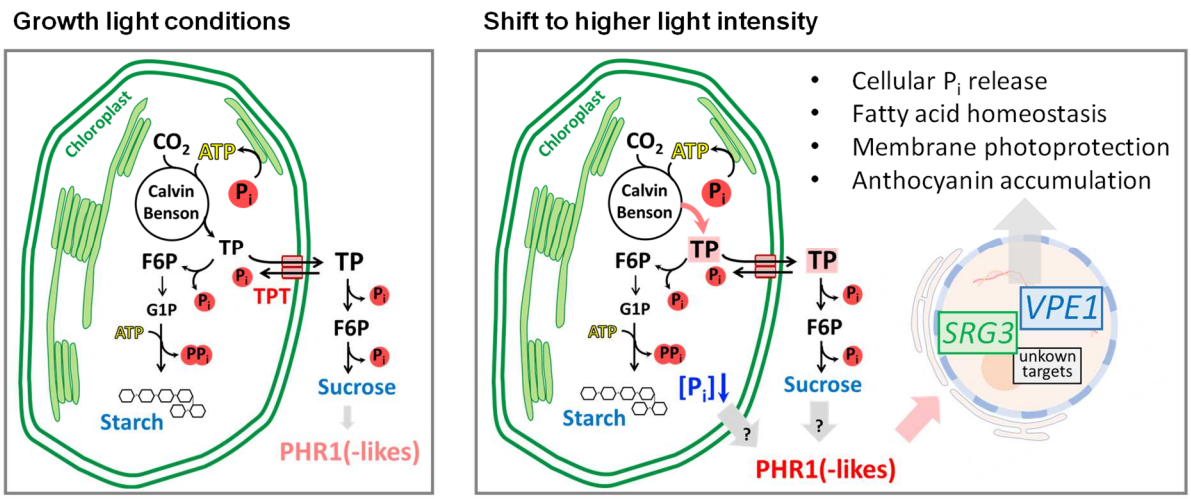

1355

1356 **Figure 6** Model of P_i signaling under light increase. **Left**, Under normal growth light
1357 conditions, production of triose phosphates in the Calvin Benson cycle and their utilization in
1358 downstream processes such as starch and sucrose biosynthesis are balanced, and the rate of P_i
1359 recycling matches its consumption by the chloroplast metabolism (Stitt *et al.*, 1987; McClain
1360 & Sharkey, 2019). **Right**, Upon shift to higher fluence rates, phosphorylated photosynthetic
1361 intermediates accumulate (Borghi *et al.*, 2019), resulting in a decrease of chloroplast P_i
1362 concentrations. Chloroplast P_i levels or changes in the pools of photosynthetic products
1363 generate a signal that leads to PHR1(-like) activation. This causes P_i-starvation responsive gene
1364 expression including the induction of *SRG3* and *VPE1*, leading to P_i release from intracellular
1365 pools, and changes in lipid metabolism enabling the containment of free fatty acids and
1366 xanthophyll cycle operation, as well as anthocyanin accumulation in the medium-term. **TP**,
1367 triose phosphate; **F6P**, Fructose 6-phosphate; **G1P**, Glucose 1-phosphate.

1368